PLASMA DYNAMICS

C. Plasma Diagnostics

Academic and Research Staff

Prof. G. Bekefi
Prof. E. V. George
Dr. P. A. Politzer

Graduate Students

R. J. Hawryluk

1. FORBIDDEN OPTICAL TRANSITIONS IN A DENSE LASER-PRODUCED PLASMA

In a previous report[1] we compared the theoretical and experimental Stark profiles of the He 6678 allowed and the He 6632 forbidden lines. Because of uncertainties in the earlier work, the experiment has been redone more carefully. The wavelength range that we studied was increased and better data were obtained in the wings of the allowed and forbidden lines. The number of analyzed wavelengths was also increased. Data on both sides of the center of the plasma were taken and Abel-inverted to obtain the profile as a function of radial position.

The plasma was produced by a repetitively pulsed CO_2 laser which produces 1-2 MW pulses of radiation at 10.6 μ wavelength. The laser light was focused by a germanium lens onto a cell filled with spectroscopic grade helium at a pressure of ~3/4 atm. The plasma was produced by optical breakdown at the focal spot of the lens. The plasma was cigar-shaped, with its major axis along the direction of the incident laser radiation. The light from the plasma passed through a condensing lens, an optical flat, and was focused onto the entrance slits of the spectrometer. Scanning perpendicular to the major axis was achieved by rotating the flat optical plate. This focused different transverse positions onto the entrance slits of the spectrometer. The light from the helium plasma was focused onto the slits of a 0.5 m scanning spectrometer provided with a motor-driven wavelength scan (Jarrell-Ash, Model 82-020) and photomultiplier output. The output from the photomultiplier tube was fed into an oscilloscope and a boxcar integrator and from there into a strip-chart recorder. The 250-ns gate width of the boxcar integrator was the time resolution of the experiment. The time delay could be set at any time in the afterglow of the plasma. All measurements for the data presented here were made at 5 μs in the afterglow of the plasma.

Detailed spatial and temporal properties of the plasma have been reported

*This work was supported by the U.S. Atomic Energy Commission (Contract AT(11-1)-3070).

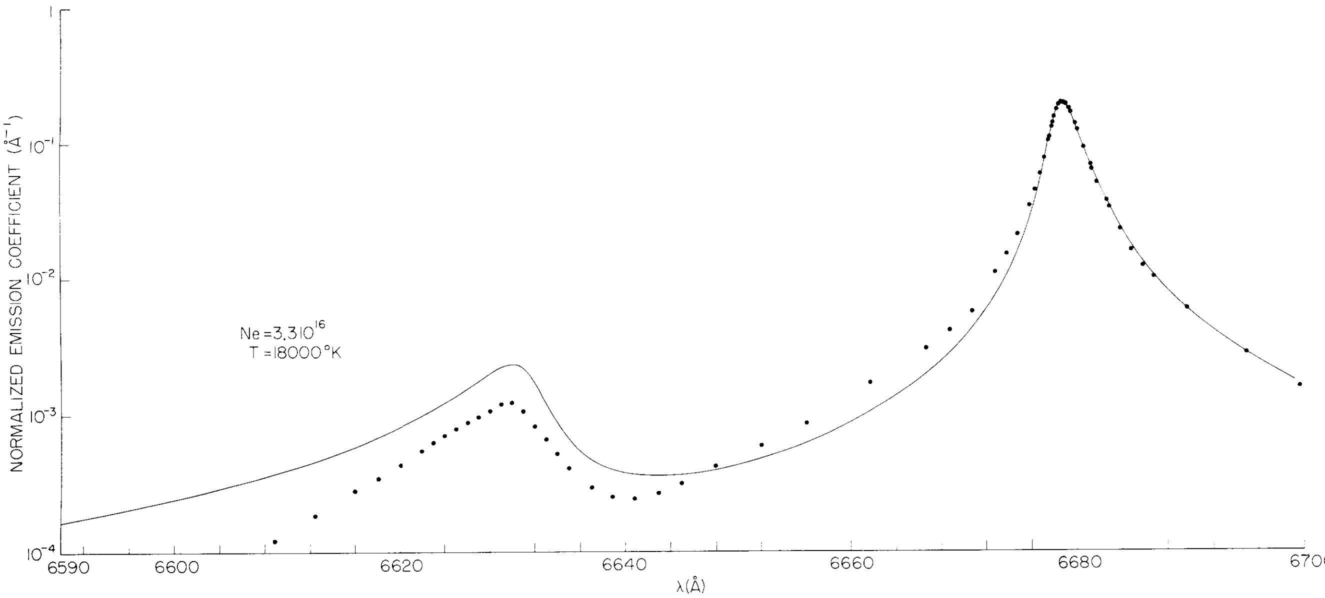

Fig. VII-1. Line profile of the He 6678 allowed line and its forbidden component. Points are the Abel-inverted experimental profile at 1.1 mm radial distance from the plasma axis. Solid line is the best-fit theoretical profile to the allowed line corresponding to $N = 3.3 \times 10^{16}$ cm^{-3} and $T = 18,000°K$.

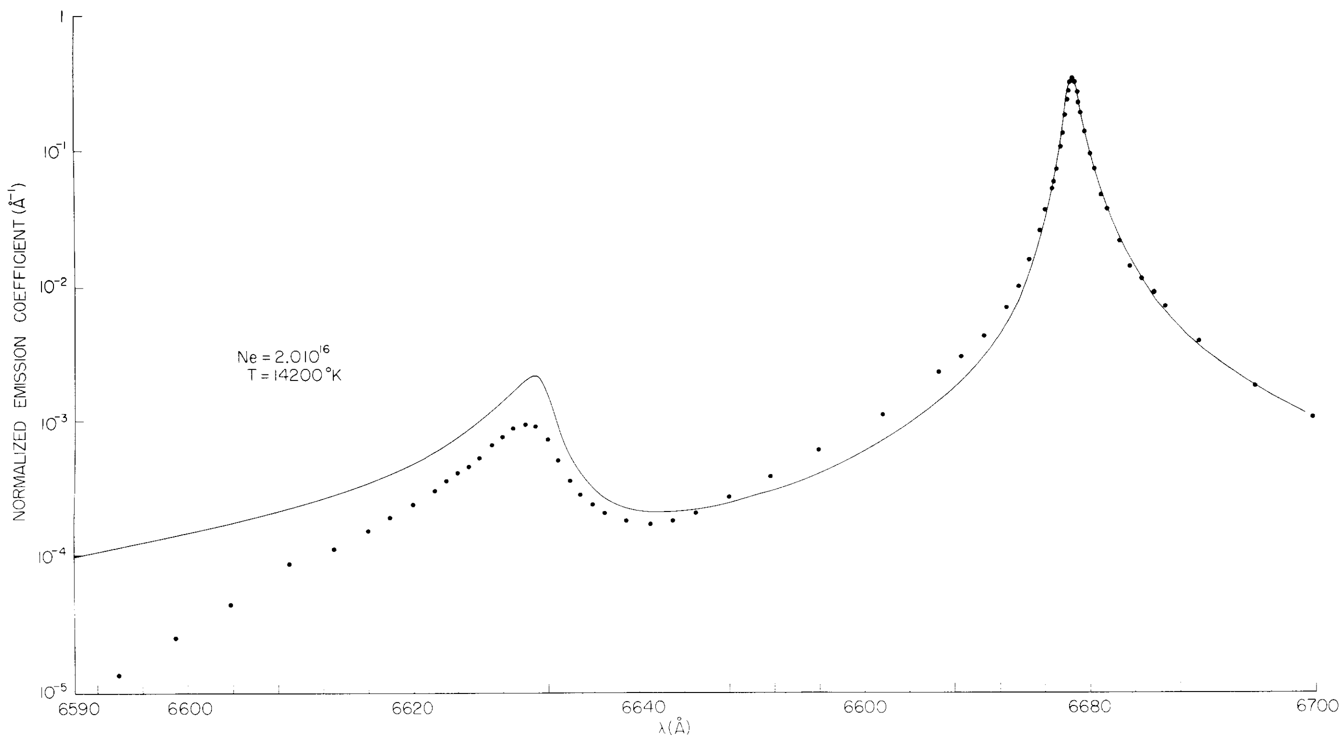

Fig. VII-2. Line profile of the He 6678 allowed line and its forbidden component. Points are the Abel-inverted experimental profile at 1.7 mm radial distance from the plasma axis. Solid line is the best-fit theoretical profile to the allowed line corresponding to $N = 2.0 \times 10^{16}$ cm^{-3} and $T = 14,200°K$.

elsewhere.[2] We have found that the neutral helium lines are emitted preferentially from the cool, outer cylindrical gas shell. The shell surrounds a hot, dense core that emits predominantly ionic lines. The plasma is quite symmetric about the major axis of the cigar and therefore Abel inversion of the results is appropriate. An examination of the optics used in this experiment showed that the use of the optical plate to move the image vertically is justified.[3]

One of the results of the present study has been to determine the temperature in the cool outer halo of the plasma. The temperature in the halo, as a function of radial position, was found from the ratio of the Abel-inverted intensity of the neutral He 4713 line and the He 6678 line to the intensity of the continuum in a 100 Å band centered about the line. The use of larger wavelength scans enabled us to determine the temperature in the halo with more accuracy than in our previous report.

At the time of observation, 5 μs in the afterglow, the He 6678 line is found to be mildly self-absorbed (~20%). To show this, light emitted by the plasma in the direction away from the spectrometer slits is reflected back into the plasma by means of a spherical mirror. Measurements of the relative increase in the spectrometer output give the absorptivity of the medium.

A detailed study of the line profile of the Abel-inverted He 6678 (2^1P-3^1D) allowed line and the He 6632 (2^1P-3^1D) forbidden transition was performed at two radial positions in the cool outer halo. The resulting profiles are shown in Figs. VII-1 and VII-2. From the computer code used previously,[1] we obtained the best-fit theoretical curve, using the conventional theory. The temperature values were obtained from the integrated intensity of the line-to-continuum measurement. We found that at r = 1.1 mm, T = 18,000°K, and at r = 1.7 mm, T = 14,200°K. The density was varied in 0.1×10^{16} cm^{-3} increments. Theoretical curves corresponding to different densities were plotted on semi-log paper and were positioned to obtain the best fit to the experimental data in the vicinity of the allowed line. Through the use of larger wavelength scans, we were able to fit the He 6678 line to the conventional theory in the wings of the line. Thus our analysis was not dependent upon the peak of the He 6678 line, which, as we have discussed previously, could have been self-absorbed.

The conventional theory gives excellent agreement in the red wing of the allowed line. Large discrepancies with the conventional theory are found in the vicinity of the forbidden line, which cannot be accounted for merely by varying the temperature or the density of the plasma.

Our dynamic correction factors are obtained by use of Griem's theory,[4] as calculated by Ya'akobi et al.[1] In Table VII-1 R_{COR}, which is the value by which the conventional theory should be multiplied to account for ion dynamics, is compared with R_{EXP}, which is the ratio of the experimental intensity to the intensity predicted by the conventional theory. There is good agreement between theory and experiment at λ_2, which

Table VII-1. Comparison of R_{EXP} with R_{COR}.

Radial Position = 1.1 mm $N_e = 3.3 \times 10^{16}\ cm^{-3}$ T = 18,000°K			
	$\lambda_1(6630)$	$R_{EXP} = 0.51$ $R_{COR} = 0.60$	Discrepancy = 17.6%
	$\lambda_2(6654.4)$	$R_{EXP} = 1.35$ $R_{COR} = 1.46$	Discrepancy = 8.1%
Radial Position = 1.7 mm $N_e = 2.0 \times 10^{16}\ cm^{-3}$ T = 14,200°K			
	$\lambda_1(6631.7)$	$R_{EXP} = 0.44$ $R_{COR} = 0.51$	Discrepancy = 15.9%
	$\lambda_2(6655)$	$R_{EXP} = 1.33$ $R_{COR} = 1.37$	Discrepancy = 3.0%

is midway between the allowed line and forbidden line. At the peak of the forbidden line, there are still discrepancies, 17.6% and 15.9% for the two radial positions, respectively. Nonetheless, the ion dynamic correction factor significantly improves the agreement between theory and experiment.

Previously, we reported good agreement at the center of the forbidden line and not as good agreement at the midpoint. In the present experiment, through the use of the line-to-continuum measurement, we have better data on the temperature in the halo. The use of the observed lower temperature accounts for the change in our conclusions. Figures VII-1 and VII-2 also show the poor agreement in the blue wings of the forbidden line. For sufficiently large values away from the center of the forbidden line, the ion dynamic correction factor should be negligible and the results of the experiment should agree well with the conventional theory. We see that the experimental values diverge from the theoretical profiles instead of asymptotically approaching them. Thus the integrated intensity of the forbidden line is less than predicted by either the conventional theory or the conventional theory with ion dynamics. Indeed, it is interesting to note that Lee[5] found in his improved calculations that the integrated intensity of the He 4470 forbidden line did change because of ion dynamics.

Other questions arise when using the ion dynamic formalism. The ion dynamic correction factors should be important mainly near the center of the forbidden line and not in the wings. Yet the correction at the midpoint is quite appreciable and good agreement between theory and experiment is obtained.

It appears that a complete understanding of the line profile awaits a more comprehensive theory, which would allow the integrated intensity of the forbidden line to change and shifts of the forbidden line to occur because of ion dynamics.

R. J. Hawryluk

References

1. B. Ya'akobi, E. V. George, G. Bekefi, and R. J. Hawryluk, Quarterly Progress Report No. 102, Research Laboratory of Electronics, M.I.T., July 15, 1971, pp. 67-79; also "Stark Profiles of Forbidden and Allowed Transitions in a Dense, Laser-Produced Helium Plasma" (to appear in J. Phys. B (Atomic and Mol. Phys.)).
2. E. V. George, G. Bekefi, and B. Ya'akobi, Phys. Fluids 14, 2708 (1971).
3. R. J. Hawryluk, S.M. Thesis, Department of Physics, M.I.T., May 1972.
4. H. R. Griem, Comments on Atomic Molecular Phys. 3, 24-27 (1971).
5. R. W. Lee, J. Phys. B. (Atomic and Mol. Phys.) 5, 23 (1972).

E. Feedback Stabilization

Academic Research Staff

Prof. R. R. Parker
Prof. L. D. Smullin
Prof. K. I. Thomassen

Graduate Students

S. P. Hirshman
R. S. Lowder
A. R. Millner

1. ION-ABLATION DRAG MODEL FOR A COAXIAL PLASMA GUN

In our last report,[1] we showed how a simple snowplow slug model for an accelerating current sheet might be sufficient for analysis of the dynamics of a coaxial plasma gun. In addition to the usual snowplow pressure, we postulated an effective ion drag force resulting from the loss of ion momentum as the ion flux at the cathode scatters and loses (on the average) its axially directed velocity component. Under the assumption that secondary processes at the electrode could be neglected, it follows by charge conservation that the current at the cathode is entirely attributable to the ions; hence, the rate at which axial momentum is lost to the sheet is $g \frac{|I|}{e} m_i u_s$, where $g \leq 1$ is a geometrical factor depending only on the details of the scattering process at the cathode surface.

It has been found that such a drag force is not large enough to account for the experimentally observed velocities in coaxial guns.[2] Furthermore, it cannot account for the fact that a variety of different gases exhibit roughly similar final velocities when observed experimentally.[3] It seems that a drag force depending on some "external" parameter, for example, acceleration of the electrode material, might be responsible for the observed limiting velocities. A two-step process is proposed in which the cathode ion current causes sputtering of the metallic material (as in typical cathode-arc sputtering), and the resulting ionization and acceleration of this heavy material results in the "ion-ablation" drag force. Presumably, this force would be more important in negative-inner electrode operation, since the ions would be accelerated in a stronger field ($E_z \sim 1/r^2$) and there would be more drag on the current sheet. Since the force would also be dependent on the mass (M_{ab}) of the sputtered metal, it might predict the observed limiting velocities.

*This work was supported by the U.S. Atomic Energy Commission (Contract AT(11-1)-3070).

If we combine this drag component with the sheet momentum equation and neglect the (usually) small snowplow pressure, we obtain

$$M \frac{du}{dt} + g\left(1 + f\frac{m_{ab}}{m_i}\right)\frac{|I|}{e} m_i u = \frac{1}{2}\mathscr{L} I^2, \tag{1}$$

where f is the effective coefficient of sputtering given by $f \equiv j_{sp}/j_i$. It can be shown that this equation is valid only when $u \sim 2^{1/2} u_a$ or $\left(1 - 2u_a^2/u^2 \ll 1\right)$, where u_a is the Alfvén velocity for waves in the sheet. This condition will be valid only near the cathode; hence, the momentum equation (1) is an approximation that is valid only for negative-inner electrode operation. Note that the correct ablation contribution for $u \geq 2^{1/2} u_a$ is actually

$$f_{ab} = g f \frac{m_{ab}}{m_i}\left(1 - \sqrt{1 - \frac{2u_a^2}{u^2}}\right)\frac{|I|}{e} m_i u$$

$$u_a \equiv \frac{B^2}{\mu_o n_i m_i}.$$

Thus, for $f \gtrsim m_i/m_{ab}$, this can be an important contribution to the total sheet drag force.

Figures VII-3 through VII-5 give a comparison of theoretical calculations based on Eq. 1 and our circuit model presented in Quarterly Progress Report No. 105 with experimental data of Burkhardt and Lovberg.[2] For the calculations based on Eq. 1 we chose $g = 1/2$ and $f\frac{m_{ab}}{m_i} = 4.5$. Clearly, for $\frac{m_{ab}}{m_i} \gg 1$, this indicates that only a relatively small fraction of metal atoms need be sputtered and accelerated to produce the required drag force.

In all of our work thus far, we have neglected internal plasma resistive effects in the energy equations (formally equivalent to Kirchhoff's voltage law[4]) under the assumption that they are small and hence would produce a small plasma resistance (compared with dL/dt, for example). By forming $J \cdot E = \frac{\partial}{\partial t}\sum_k n_k\langle\frac{1}{2} mv_k^2\rangle + \nabla \cdot \sum n_k\langle\frac{1}{2} mv^2\bar{v}\rangle_k + \Gamma_{rad}$ and writing $\bar{v} = \bar{u} + \bar{v}_r$, we can integrate it over the plasma volume and identify those portions not directly related to the power input into bulk acceleration. (Care must be taken to write $J = \sigma(E+u\times B)$ and separate $J \cdot E = J^2/\sigma + u \cdot (J\times B)$ into a dissipative term and an $F \cdot u$ power term.) Then, with $\int J^2/\sigma\, dv \equiv RI^2$, after some calculation, we find

$$RI^2 = R_p I^2 + e\phi_i\left[\frac{1}{m_i}\frac{dM}{dt} + \frac{g|I|}{e}\right] + BT_e^{1/2} - u^2\frac{dm_s}{dt} + |I|V_c + \frac{3}{2}k\left[(T_e+gT_i)\frac{|I|}{e}\right]$$

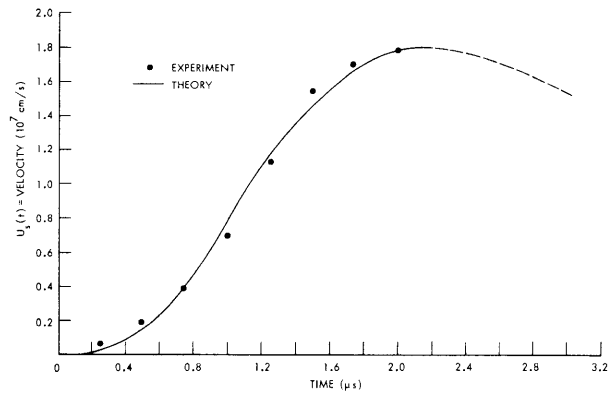

Fig. VII-3. Current-sheet velocity, $u_s(t)$. Experimental points from Burkhardt and Lovberg.[2]

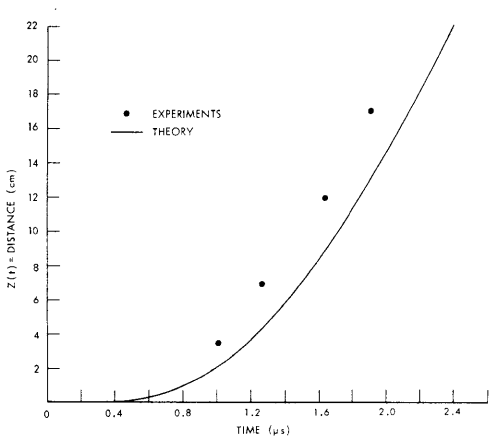

Fig. VII-4.
Sheet position $z(t) = \int_0^t u_s(t)\,dt$. Experimental points from Burkhardt and Lovberg.[2]

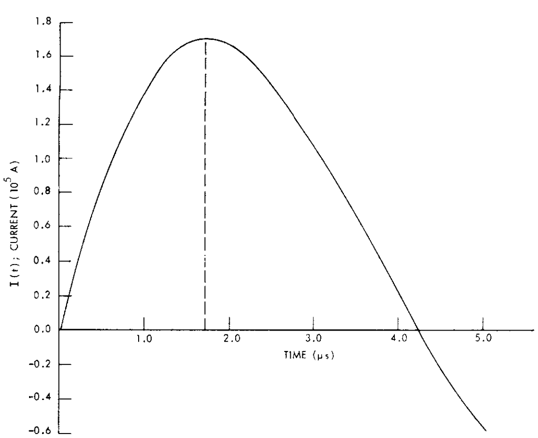

Fig. VII-5.
Capacitor current I(t) (theoretical).

and $R_p \cong$ "classical" plasma resistance (a function of T_e, T_i). Here the terms containing the ionization potential ϕ_i represent power losses caused by ionization of incoming gas and re-ionization of gas reflected at the walls. The term $BT_e^{1/2}$ represents losses from electron Bremsstrahlung radiation. Other radiative terms (such as recombination) have been neglected. The $u^2 \frac{dm_s}{dt}$ term is derived from the inelastic collisions of the incoming ions with the sheet. As compared with the energy E_o initially stored in the capacitor bank, $W = \int_0^\infty RI^2 \, dt$ is seen to be small. For instance, $\int_0^\infty \frac{e\phi_i}{m_i} \frac{dM}{dt} \, dt \sim$ 10 joules (for $M_f = 10^{-8}$ kG) $\ll 10^3$ joules. Moreover, the power terms that are due to ionization will only be significant ($\approx 10^8$ W) near t = 0, when d/dt is large. Since we are not concerned with modeling the initial breakdown processes, we conclude that the neglect of resistive terms in the circuit equation is justified.

We shall continue to elaborate on the proposed ion-ablation drag model. A more detailed study of the surface (cathode) phenomenon is now warranted and, we hope, will lead to a justification of the use of this model. When the validity of this model has been ascertained, new calculations of efficiency may be made with new predictions obtained for more efficient modes of gun operation.

S. P. Hirshman, L. D. Smullin

References

1. S. P. Hirshman and L. D. Smullin, "Investigation of a Plasma Gun," Quarterly Progress Report No. 105, Research Laboratory of Electronics, M.I.T., April 15, 1972, pp. 89-93.
2. L. Burkhardt and R. Lovberg, "Current Sheet in a Coaxial Plasma Gun," Phys. Fluids 5, 341-347 (1962).
3. J. Keck, "Current Speed in a Magnetic Annular Shock Tube," Phys. Fluids Supplement 7, S16 (1964).
4. C. J. Michels, et al., "Analytical and Experimental Performance of Capacitor Powered Coaxial Plasma Guns," AIAA J. 4, 823 (1966).

2. FEEDBACK STABILIZATION OF KINK MODES INCLUDING THE INFLUENCE OF NEGATIVE-ENERGY MODES

Extension of the Energy Principle to Include Feedback Magnetic Fields

We shall extend the energy principle of Bernstein, Frieman, Kruskal, and Kulsrud[1] to include the effects of externally imposed feedback magnetic fields.

First we outline the energy principle and show how it applies to feedback stabilization. Then we find the wave potential energy in terms of the wave displacement vector $\underline{\xi}$, where $\underline{\xi}$ is a function of (r, θ, z). A relatively simple expression for the wave potential energy results from using the appropriate form of $\underline{\xi}(r, \theta, z)$. From this expression we then obtain the feedback field required for stability.

a. On the Energy Principle

Consider a current-carrying cylindrical plasma column having a boundary at $r = a$, with vacuum between $r = a$ and the surrounding conducting walls and/or feedback coils, as shown in Fig. VII-6. In the absence of waves (or in the zero-order state), there is a certain amount of zero-order potential energy, W (magnetic field energy), and kinetic energy, K, stored within the plasma boundary. In the presence of a wave, W and K change in amounts δW and δK. Here, δK is the gain in particle kinetic energy as the particles move in response to the wave electric field. In the zero-momentum frame that we use here, δK is positive.

If δW is also positive, then the net change in total energy, $\delta W + \delta K$, is positive. Thus these waves are stable propagating waves, since for such waves to grow they would have to be driven by an external energy source to provide the increase in $\delta W + \delta K$.

If δW is negative, $\delta W + \delta K$ can be zero, and thus spontaneous growth (or decay) of these modes would be allowed without requiring an external energy source (or sink). For example, a growing unstable kink mode generates currents; these currents reduce the stored magnetic energy, thereby providing a source of kinetic energy for the ions, which are accelerating as the wave grows.

Thus a particular wave will not be an exponentially growing mode if the associated potential energy change δW is positive. From this energy-principle viewpoint, the role of feedback is to modify δW so that δW is always positive.

It is customary to break up δW into three components,

$$\delta W = \delta W_f + \delta W_s + \delta W_v. \tag{1}$$

Here, δW_f is the increase within the plasma boundary, δW_s is a surface term that occurs only if there is a sheet current at the plasma boundary, and δW_v is the net energy loss from the plasma region to the vacuum region. δW_f depends both on the amplitude of the wave displacement $\underline{\xi}$ at the boundary of the plasma and on the r, θ, and z dependence of $\underline{\xi}$ away from the boundary. δW_s and δW_v depend only on the wave amplitude at the boundary. Each of these components of δW can be computed if we know the spatial form of $\underline{\xi}(r, \theta, z)$. The trick for finding the appropriate spatial form is to use the expression for δW in terms of $\underline{\xi}$ to find the particular perturbation that minimizes δW. By using this particular displacement, we can find the minimum value of δW.

Externally imposed feedback magnetic fields (fields arising from external feedback currents) can be used to ensure that this minimum value of δW is positive. In particular, only δW_v depends on these feedback fields; both δW_s and the minimized value of δW_f are independent of the feedback field (at least at marginal stability). Thus if δW is negative in the absence of feedback, then feedback can be used to increase δW_v sufficiently to make $\delta W_f + \delta W_s + \delta W_v > 0$.

The final form of δW_v given by Bernstein, Frieman, Kruskal, and Kulsrud[1] is an integral over the vacuum region of the perturbed magnetic field energy. One of their intermediate expressions is more appropriate, however, for our purposes,

$$\delta W_v = \frac{1}{2\mu_o} \int d\sigma\, (\underline{n} \cdot \underline{\xi})\hat{\underline{B}} \cdot \text{curl } \underline{A}, \tag{2}$$

which is a surface integral over the plasma boundary. Here, $d\sigma$ is a surface element, $\underline{n}$ is the outward normal, $\hat{\underline{B}}$ is the vacuum value of the zero-order magnetic field, and $\underline{A}$ is the perturbed magnetic vector potential. This expression for δW_v can be shown to be just the time integral from $t = -\infty$ to $t = t$ of the Poynting flow, $\frac{1}{\mu_o} \tilde{\underline{E}} \times \tilde{\underline{B}}$, integrated over the plasma surface. It is this flow of energy from the plasma region into the vacuum region that can be increased by the feedback fields to increase the stability of the system.

b. Problem

The particular plasma considered here is a cylindrical plasma column having its boundary at $r = a$. The plasma carries axial and azimuthal currents, the radial distribution of the current is arbitrary but is in keeping with the equilibrium requirement $\underline{j} \times \underline{B} = \nabla p$, where p is the pressure, and $\underline{j}$ is the current density.

The kink modes and the feedback system are shown in Fig. VII-6. The kink modes are helical perturbations about the plasma column. The helical coils have the same pitch as the perturbation. The feedback currents carried by these distributed coils are spatially and temporally like the image currents on a conducting wall, except that the relations of their amplitude and phase with respect to the plasma perturbation are now kept arbitrary.

The feedback field B_f is shown in Fig. VII-7. B_f is the azimuthal component at $r = a$ of the vacuum value of the feedback magnetic field, which is the field arising from all external feedback currents (including image currents on conducting walls). For a current K_f in the feedback coils, B_f is the vacuum field produced by K_f plus the field produced by associated image currents on nearby walls.

We give our results in terms of B_f requirements. Thus these results can be applied to any particular feedback system for sensing the wave and for applying the required B_f. (The B_f requirements themselves do not depend on such external geometry considerations but only on the plasma parameters.)

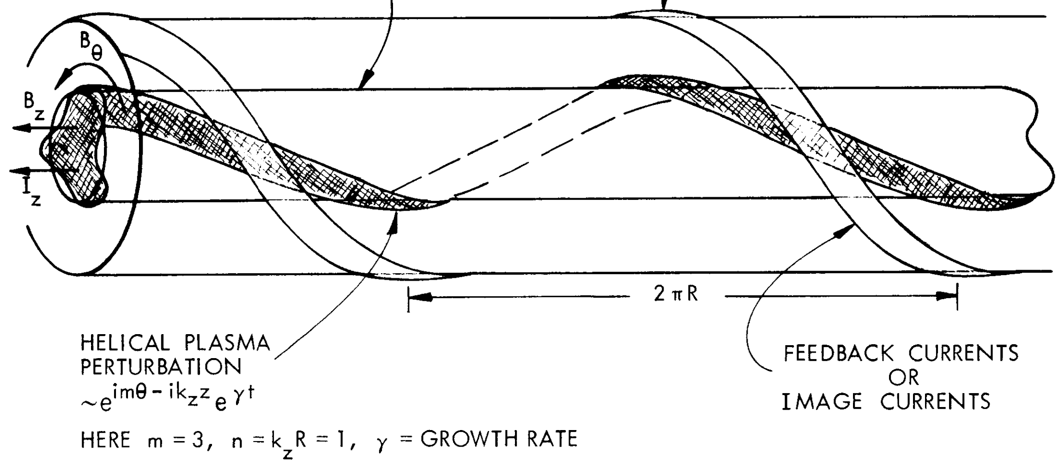

Fig. VII-6. Kink modes and feedback system.

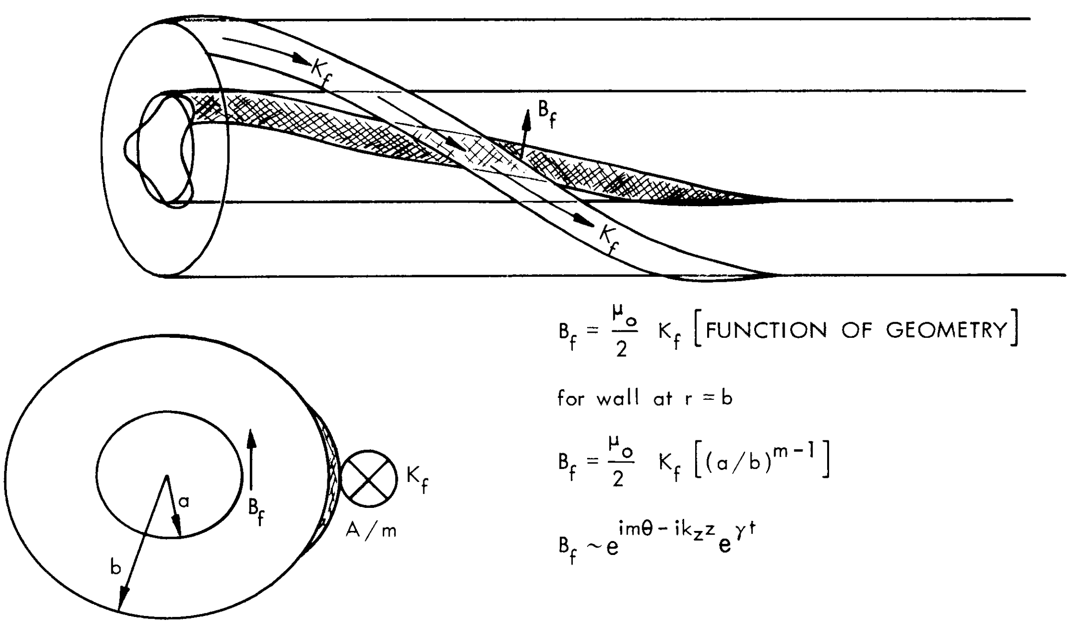

Fig. VII-7. Kink modes and feedback field. B_f is the externally produced vacuum field at $r = a$.

c. Evaluation of δW_v

In the current-free vacuum region, the perturbed magnetic field, $\tilde{\underline{B}}$, can be represented by the gradient of a scalar magnetic potential ψ,

$$\tilde{\underline{B}} = \nabla\psi \tag{3}$$

with the condition $\nabla^2\psi = 0$. There are two sets of currents producing $\tilde{\underline{B}}$, the external currents plus currents in the plasma. The field contributed by external currents has the value B_f at the plasma surface. The rest of $\tilde{\underline{B}}$ is contributed by plasma currents; the plasma current contribution will be such that its field plus the feedback field will satisfy the MHD "field-freezing" or "line-bending" condition on $\tilde{B}_r = \hat{\underline{r}} \cdot \tilde{\underline{B}}$,

$$\tilde{B}_r \Big|_{r=a} = i(k_{||} B \xi_r) \Big|_{r=a},$$

where B is the magnitude of the zero-order field $\underline{B}$, $k_{||}$ is the wave number of the wave along $\underline{B}$, and ξ_r is $\hat{\underline{r}} \cdot \underline{\xi}$, with $\hat{\underline{r}}$ a unit vector.

Thus knowing the fields arising from external currents and from internal plasma currents, we can solve for the field in between these sets of currents and obtain

$$\psi = -\frac{a}{m}\begin{bmatrix} i(k_{||}B\xi_r)\big|_{r=a} \\ +iB_f \end{bmatrix}\left(\frac{a}{r}\right)^m - \frac{a}{m}\left[iB_f\right]\left(\frac{r}{a}\right)^m.$$

We have taken both sets of currents to be distributed as $\exp(im\theta+ik_z z)$, where m is the azimuthal wave number. The $(a/r)^m$ and $(r/a)^m$ are $k_z \ll \frac{m}{a}$ expansions of the more correct m^{th}-order Bessel functions $K_m(k_z r)/K_m(k_z a)$ and $I_m(k_z r)/I_m(k_z a)$, respectively.

Relating our results to a torus of radius R by letting $k_z = -\frac{n}{R}$, and defining

$$B_a = B_\theta \big|_{r=a}$$

$$q_a = (rB_z/RB_\theta)\big|_{r=a} = aB_z/RB_a$$

$$\xi_a = \xi_r \big|_{r=a} = \xi_{ao} \exp(im\theta+ik_z z+\gamma t),$$

where γ is the growth rate, we have

$$\psi = \left[-\frac{a}{m}\left\{i\frac{B_a}{a}(m-nq_a)\xi_a + iB_f\right\}\right]\left(\frac{a}{r}\right)^m + \left[-\frac{a}{m}\{iB_f\}\right]\left(\frac{r}{a}\right)^m. \tag{4}$$

Thus, for δW_v (Eq. 2), we have

$$\delta W_v = \frac{1}{2\mu_o} \int d\sigma\ \xi_a(\hat{\underline{B}} \cdot \nabla\psi)$$

$$= 2\pi R\ \frac{1}{2\mu_o} \int_0^{2\pi} a\ d\theta\ \xi_a B k_{\|}\psi,$$

where the $2\pi R$ is the associated torus perimeter. Using this value of ψ, we obtain

$$\delta W_v = W_o \left[(m-nq_a)^2 + 2(m-nq_a)\ \frac{B_{fo}}{B_a \frac{\xi_{ao}}{a}} \right], \tag{5}$$

where

$$W_o = 2\pi R(\pi a^2)\ \frac{B_a^2}{2\mu_o} \left(\frac{\xi_{ao}^2}{a^2}\right) \frac{1}{m} \tag{6}$$

and W_o is approximately $\frac{1}{m}(\xi_{ao}/a)^2$ times the energy stored in the poloidal magnetic field.

We see that for $B_f = 0$, δW_v is just $(m-nq_a)^2\ W_o$. With feedback present, B_f/ξ_a can be increased to make δW_v larger, and hence to overcome negative contributions from δW_f and δW_s, the other parts of δW.

d. Surface Term

The surface term δW_s is an integral over the plasma surface and, as given by Bernstein et al.,[1]

$$\delta W_s = -\frac{1}{2} \int d\sigma\ (\underline{n} \cdot \underline{\xi})\underline{n} \cdot \left\langle \text{grad}\left(p + \frac{|B|^2}{2\mu_o}\right) \right\rangle.$$

Here $\left\langle \text{grad}\left(p + \frac{|B|^2}{2\mu_o}\right) \right\rangle$ is the jump at $r = a$ in the gradient of the pressure plus magnetic field energy density. Such a jump at $r = a$ occurs only if there is a sheet current at $r = a$. If I_z is the total axial current and $(1-f)I_z$ is the axial sheet current at $r = a$ producing the jump in $p + \frac{|\underline{B}|^2}{2\mu_o}$, then we obtain[2]

$$\delta W_s = -W_o[(1-f^2)m], \tag{7}$$

where m is the azimuthal mode number, and W_o is as defined above.

For skin pinches δW_s is the destabilizing term, but often there is no skin current and (1-f) and δW_s are zero.

e. Interior Term

The evaluation of δW_f depends on the spatial dependence of $\underline{\xi}$ within the plasma, while δW_s and δW_v only depend on the amplitude of the perturbation at the plasma boundary.

One way to compute δW_f is to make a reasonable guess about what $\underline{\nabla} \cdot \underline{\xi}$ is and how $\underline{\xi}$ varies with radius. Several guesses may give an estimate of how negative δW_f might be, and hence guessing is not without merit.

Of greater interest is the spatial form for $\underline{\xi}(r, \theta, z)$ which gives δW its minimum value. There is also a spatial form that minimizes $\delta W - \delta K$ or $\delta W/\delta K$, and this is not necessarily the same form that minimizes δW. For feedback stabilization purposes, however, we are interested only in finding the spatial form that minimizes δW_f, and hence that minimizes δW. Then we shall know how large B_f must be so that the minimized δW is positive.

The increase in perturbed energy within the plasma boundary, δW_f, is given by Bernstein et al.[1] as

$$\delta W_f = \frac{1}{2\mu_o} \int d\tau \; |\underline{Q}|^2 - \frac{1}{2\mu_o} \int d\tau \; \underline{j} \cdot \underline{Q} \times \underline{\xi}$$
$$+ \frac{1}{2} \int d\tau \left[\gamma_s p (\text{div } \underline{\xi})^2 + \text{div } \underline{\xi} \; (\underline{\xi} \cdot \text{grad } p) \right], \tag{8}$$

where γ_s is the specific heat ratio, $d\tau$ denotes volume integration over the plasma volume, and

$$\underline{Q} \equiv \underline{\nabla} \times (\underline{\xi} \times \underline{B}).$$

For an ideal MHD plasma, such as we have assumed, $\underline{Q}$ is the perturbed magnetic field.

As Newcomb[3] has shown, δW_f can be partially minimized with respect to ξ_θ and ξ_z, to leave δW as a radial integral involving only the radial component of $\underline{\xi}$. Newcomb's minimization conditions for ξ_θ and ξ_z are more interesting when expressed as conditions on ξ_k and $\xi_{r\times k}$, the components along and perpendicular to $\underline{k}$. That is, we can write

$$\underline{\xi} = \hat{\underline{r}}\xi_r + \hat{\underline{\theta}}\xi_\theta + \hat{\underline{r}} \times \hat{\underline{k}}\xi_{r\times k},$$

where

$$\underline{k} = \hat{\underline{\theta}}\left(\frac{m}{r}\right) + \hat{\underline{z}}\left(\frac{-n}{R}\right) = \hat{\underline{k}}k.$$

(Note: For this definition of $\underline{k}$ or of n, the condition (m−nq = 0) corresponds to $\underline{k} \cdot \underline{B} = 0$.)

The conditions that partially minimize δW_f are

$$\xi_k = i\left(\frac{1}{kr}\right)\frac{d}{dr}(r\xi_r)$$

and

$$\xi_{r\times k} = i\left(\frac{2}{m-nq}\right)\left(\frac{n/R}{k}\right)\xi_r.$$

The first minimization condition corresponds to taking $\nabla \cdot \underline{\xi} = 0$. The second condition breaks down as (m−nq) becomes much smaller than $\frac{n/R}{k}$.

Using these values of ξ_k and $\xi_{r\times k}$, we obtain δW_f as an integral involving only ξ_r,

$$\delta W_f = W_o \int_0^a dr \left(\frac{B_\theta/r}{B_a/a}\right)^2 \left(\frac{2mr}{a^2\xi_{ao}^2}\right) g, \tag{9}$$

where

$$g = \begin{bmatrix} (m-nq)^2 & \times \frac{1}{2}\left\{\xi_{ro}^2 + \left(\frac{1}{k^2r^2}\right)\left[(r\xi_{ro})'\right]^2\right\} \\ -2(m-nq) & \times \xi_{ro}\left(\frac{m}{k^2r^2}\right)(r\xi_{ro})' \\ -\bar{j}_z' r/\bar{j}_z & \times \xi_{ro}^2 \\ -2(n/kR)^2 & \times \xi_{ro}^2 \end{bmatrix}$$

The prime denotes $\partial/\partial r$, and $\bar{j}_z$ is the average from r = 0 to r = r of j_z, with $\bar{j}_z$ and $\bar{j}_z'$ functions of r.

One reason for writing δW_f in this particular form is that it quickly gives the constant current density result. That is, for $\bar{j}_z' = 0$ and $(n/R)^2 \ll k^2 \approx (m/r)^2$, δW_f comes simply from the first two terms. For $\bar{j}_z$ = constant, the modes are essentially surface modes with ξ_{ro} having the radial dependence $\xi_{ro} = \xi_{ao}(r/a)^{m-1}$. For $\bar{j}_z' = 0$, $B_\theta/r = B_a/a$, $(m-nq) = (m-nq_a)$, and δW_f becomes

$$\delta W_f = W_o \int_0^a dr \left(\frac{2mr}{a^2\xi_{ao}^2}\right)\left[\left\{(m-nq_a)^2 - 2(m-nq_a)\right\}\xi_{ao}^2\left(\frac{r}{a}\right)^{2m-2}\right]$$

$$= W_o\left[(m-nq_a)^2 - 2(m-nq_a)\right].$$

When combined with the δW_v result (Eq. 6) this result leads to the correct stability bounds for the constant-current case. That is, with no feedback,

$$\delta W = \delta W_f + \delta W_v = W_o \left[2(m-nq_a)^2 - 2(m-nq_a) \right].$$

Thus the plasma is unstable ($\delta W < 0$) for q_a such that $0 < (m-nq_a) < 1$.

The next step is to determine the radial dependence of ξ_{ro} that minimizes δW_f. The standard procedure is to use the calculus of variations which says that the $\xi_{ro}(r)$ function that minimizes δW_f is given by the Euler-Lagrange equation

$$\frac{d}{dr} \left[\frac{\partial}{\partial \xi'_{ro}} (\mathscr{L}) - \frac{\partial}{\partial \xi_{ro}} (\mathscr{L}) \right],$$

where $\mathscr{L}$ is the integrand of δW_f. This leads to the following equation

$$r^2(r\xi_{ro})'' + C_1 r(r\xi_{ro})' + C_2(r\xi_{ro}) = 0, \tag{10}$$

where

$$C_1 = 1 + \frac{2m}{m-nq} \left[\frac{\bar{j}_z' r}{\bar{j}_z} + \frac{nq}{m} \left(\frac{\mu_o j_\theta r}{B_z} \right) - \frac{k_z^2}{k^2} \left(\frac{m-nq}{m} \right) \right]$$

$$C_2 = -\left\{ m^2 + k_z^2 r^2 + \frac{2m}{m-nq} \left[\frac{\bar{j}_z' r}{\bar{j}_z} + \frac{nq}{m} \left(\frac{\mu_o j_\theta r}{B_z} \right) - 2 \frac{k_z^2}{k^2} \right] \right\} - \frac{k_z^2 r^2}{(m-nq)^2} \left(\frac{r \frac{\partial}{\partial r} p}{B_\theta^2/2\mu_o} \right).$$

Here j_z and j_θ are the axial and azimuthal current densities, and $\left(\frac{\partial}{\partial r} p\right)$ is $j_\theta B_z - j_z B_\theta$ or $j_\perp B$.

The coefficients C_1 and C_2 are specified once the radial distributions of $j_\parallel$ and $j_\perp$ are specified (or once the pressure and the electric field along $\underline{B}$ are specified.)

This equation determines L_r, which we shall use extensively,

$$\frac{1}{L_r} \equiv \left. \frac{(r\xi_{ro})'}{(r\xi_{ro})} \right|_{r=a}, \tag{11}$$

where $(r\xi_{ro})$ is the solution to the Euler-Lagrange equation (Eq. 10), subject to the boundary conditions that ξ_{ro} be ξ_{ra} at $r = a$ and bounded at $r = 0$, and L_r is the fall-off distance of $r\xi_{ro}$ looking into the plasma from $r = a$.

A simplification occurs on integrating δW_f by parts. This simplification applies only to perturbations $\xi_{ro}(r)$ that satisfy the Euler-Lagrange equation (Eq. 10). Of course, those are the perturbations in which we are interested. We write δW_f as the sum of two integrals

$$\delta W_f = W_o \int_0^a dr \left(\frac{B_\theta/r}{B_a/a}\right)^2 \left(\frac{2mr}{a^2\xi_{ao}^2}\right)\left[\left\{\frac{(m-nq)^2 \frac{1}{2m}(r\xi_{ro})' - (m-nq)\xi_{ro}}{k^2r^2/m^2}\right\}\left(\frac{r\xi_{ro}}{m}\right)'\right]$$

$$+ W_o \int_0^a dr \left(\frac{B_\theta/r}{B_a/a}\right)^2 \left(\frac{2mr}{a^2\xi_{ao}^2}\right)\left[\begin{matrix}(m-nq)^2 \frac{1}{2}\xi_{ro}^2 - \frac{m^2}{k^2r^2}(m-nq)\xi_{ro}\frac{(r\xi_{ro})'}{m} \\ \\ -\left(\bar{j}_z' r/\bar{j}_z\right)\xi_{ro}^2 - 2(n/kR)^2\xi_{ro}^2\end{matrix}\right]. \qquad (12)$$

Integration by parts of the first integral gives

$$\delta W_f = W_o \left[\left(\frac{B_\theta/r}{B_a/a}\right)^2 \frac{2mr}{a\xi_{ao}^2}\left\{\frac{m^2}{k^2r^2}\left((m-nq)^2\frac{(r\xi_{ro})'}{2m} - (m-nq)\xi_r\right)\right\}\frac{r\xi_{ro}}{m}\right]\Bigg|_{r=0}^{r=a} + I_r$$

or

$$\delta W_f = W_o \frac{m^2}{m^2 + k_z^2a^2}\left[(m-nq_a)^2 \frac{\left[(r\xi_r)'\right]\big|_{r=a}}{m\xi_{ao}} - 2(m-nq_a)\right] + I_r, \qquad (13)$$

where I_r is the remaining integral. The simplification occurs because the remaining integral I_r is zero if $\xi_r(r)$ is a solution to the Euler-Lagrange equation (Eq. 10).

So the minimized value of δW_f (Eq. 13) is just

$$\delta W_f = W_o \frac{m^2}{m^2 + k_z^2a^2}\left[(m-nq_a)^2 \frac{a/m}{L_r} - 2(m-nq_a)\right], \qquad (14)$$

where $\frac{1}{L_r} \equiv \frac{(r\xi_{ro})'}{(r\xi_{ro})}\Bigg|_{r=a}$ is determined from the Euler-Lagrange equation (Eq. 10).

Thus for zero skin current, such that δW_s is zero, and for $k_z^2a^2 \ll m^2$, we have

$$\delta W = \delta W_f + \delta W_v$$

with

$$\delta W_f = W_o\left[-2(m-nq_a) + \frac{a/m}{L_r}(m-nq_a)^2\right]$$

and

$$\delta W_v = W_o\left[(m-nq_a)^2 + 2\,\frac{B_{fo}}{\left(B_a\,\frac{\xi_{ao}}{a}\right)}(m-nq_a)\right]$$

or $\delta W > 0$ demands

$$\delta W = W_o\begin{bmatrix}(m-nq_a)^2\left(1+\dfrac{a/m}{L_r}\right)\\ -2(m-nq_a)\left(1-\dfrac{B_{fo}}{B_a\xi_{ao}/a}\right)\end{bmatrix} \geqslant 0. \tag{15}$$

For stability, B_{fo}/ξ_{ao} must be large enough that $\delta W > 0$, or (for $m - nq_a$ positive, which is the case of interest) B_{fo} must be

$$B_{fo} \geqslant B_a\,\frac{\xi_{ao}}{a}\left[1-(m-nq_a)\left(\frac{1+\dfrac{a/m}{L_r}}{2}\right)\right]. \tag{16}$$

If B_f is not exactly in phase with ξ_a, this criterion applies to the real part of B_f.

f. Feedback Requirements Including a Sheet Current

If a sheet current is present at $r = a$, then q and B_θ values inside and outside the current sheet need to be distinguished.

Let I_z be the total axial current and $(1-f)I_z$ be the fraction of I_z that is flowing in a narrow sheet at $r = a$. Then let B_a be B_θ just outside $r = a$ or

$$B_a = \frac{\mu_o I_z}{2\pi a}.$$

Then fB_a is B_θ just inside $r = a$. With this definition δW_v is expressed as before (Eq. 5), but δW_f becomes

$$\delta W_f = W_o\left[-2f(fm-nq_a) + \frac{a/m}{L_r}(fm-nq)^2\right],$$

where W_o and q_a are still given by Eq. 6; in particular, $q_a = \frac{aB_z/R}{\mu_o I_z/2\pi a}$. L_r is still given by Eq. 11.

Thus, using the δW_s and δW_v expressions from Eq. 5 and Eq. 7, we have

$$\begin{aligned}\delta W &= \delta W_f + \delta W_s + \delta W_v \\ &= W_o \left[\left\{ -2f(fm-nq_a) + \frac{a/m}{L_r}(fm-nq_a)^2 \right\} \right. \\ &\quad + \left\{ -m(1-f^2) \right\} \\ &\quad \left. + \left\{ (m-nq_a)^2 + 2\left(\frac{B_{fo}}{B_a \frac{\xi_{ao}}{a}} \right)(m-nq_a) \right\} \right]. \end{aligned} \tag{17}$$

Or the stability requirement on B_{fo} for $m - nq_a > 0$ is

$$B_{fo} \geq B_a\left(\frac{\xi_a}{a}\right) \left[\left(\frac{f(fm-nq_a) + \frac{1}{2} m(1-f^2)}{(m-nq_a)} \right) - (m-nq_a) \left(\frac{1 + \frac{a/m}{L_r}\left(\frac{fm-nq_a}{m-nq_a}\right)^2}{2} \right) \right]. \tag{18}$$

Setting $f = 1$, we can recover the previous form (Eq. 16) which is valid for no sheet current.

g. Application of Requirements to Particular Feedback Systems

These B_{fo} requirements can be applied to particular feedback systems. The simplest system is the passive one provided by a nearby conducting wall.

A conducting wall at $r = b$ senses the net radial magnetic field resulting from perturbed plasma currents plus the image currents of the wall. The image currents (which in this case produce B_{fo}) are such that $\left.\frac{\partial\psi}{\partial r}\right|_{r=b}$ is zero. Using ψ as given previously (Eq. 4), we obtain the B_{fo} produced by these image or feedback currents,

$$B_{fo} = B_a \frac{\xi_{ao}}{a}(m-nq_a) \frac{(a/b)^{2m}}{1-(a/b)^{2m}}. \tag{19}$$

Using this B_{fo} in the B_{fo} requirement (Eq. 15, under the assumption of no skin current),

$$\left[(m-nq_a)^2\left(1+\frac{a/m}{L_r}\right)-2(m-nq_a)\left(1-\frac{B_{fo}}{B_a(\xi_{ao}/a)}\right)\right]\geq 0,$$

we obtain the requirement on the ratio (a/b) needed for stability,

$$-(m-nq_a)+(m-nq_a)^2\left[\frac{1}{1-\left(\frac{a}{b}\right)^{2m}}-\frac{1-\frac{a/m}{L_r}}{2}\right]\geq 0$$

which, for $(m-nq_a)$ positive, requires that the wall be close enough that

$$\left(\frac{a}{b}\right)^{2m}\geq\frac{1-\frac{1}{2}(m-nq_a)\left(1+\frac{a/m}{L_r}\right)}{1+\frac{1}{2}(m-nq_a)\left(1-\frac{a/m}{L_r}\right)}.$$

Thus apparently for any L_r value (for any current distribution), the wall must be very close in order to stabilize modes for which $m - nq_a$ is small.

Another feedback scheme has been considered by Arsenin and Chuyanov[4] for a plasma column carrying a uniformly distributed current ($\bar{j}_z$ = constant). The condition that they imposed was

$$\left.\frac{\partial\psi}{\partial r}\right|_{r=b}=-G\left.\frac{\partial\psi}{\partial r}\right|_{r=a},$$

where G is a constant. In this system a sensor measures the total radial field at the surface of the plasma (at r = a). Then feedback currents at r = b (or outside r = b) apply a field such that the total radial field measured by sensors at r = b is G times the field measured at r = a.

To apply our stability criterion, we need to know B_{fo} in terms of G for this particular feedback system. The magnetic potential has been given. Evaluating the radial derivative of ψ (Eq. 4) at r = a and at r = b and setting $\psi'|_{r=b} = -G\psi'|_{r=a}$, we obtain B_{fo} in terms of ξ_{ao} for this system,

$$B_{fo}=B_a\left(\frac{\xi_{ao}}{a}\right)\left[(m-nq_a)\frac{(a/b)^{2m}}{1-(a/b)^{2m}}\left(1+G\left(\frac{b}{a}\right)^{m+1}\right)\right].$$

[Note that for G = 0, B_{fo} equals the B_{fo} value for a conducting wall (Eq. 19) at r = b, as it should.]

Using this B_{fo} in our stability condition, we obtain

$$-2(m-nq_a) + (m-nq_a)^2 \left[\left(1 + \frac{a/m}{L_r}\right) + 2\,\frac{(a/b)^{2m}}{1-(a/b)^{2m}}\left(1 + G\left(\frac{b}{a}\right)^{m+1}\right)\right] \geq 0$$

or the "gain" G needs to be greater than

$$G \geq \left(\frac{b}{a}\right)^{m-1}\left[\frac{1-(a/b)^{2m}}{(m-nq_a)} - 1 + \frac{\left(1 - \frac{a/m}{L_r}\right)}{2}\right]. \qquad (20)$$

Arsenin and Chuyanov found a sufficient condition for stability of the m = 1 mode in a plasma having uniform $\bar{j}_z$ (where $\frac{a/m}{L_r} = 1$) to be

$$G \geq \left[\frac{1}{m-nq_a}\right]$$

which does agree with our more general result (Eq. 21) for the same feedback system.

h. Other Feedback Systems

Other feedback systems can be envisioned. For example, an enhanced image-current system would consist of a coil sensing the total radial field at r = b and an external coil that sees only the magnetic field arising from the feedback current. The external coil could be used to subtract that part of $\tilde{B}_r$ at r = b that is due to the feedback current. The net signal from the two coils gives that part of $\left.\frac{\partial\psi}{\partial r}\right|_{r=b}$ which is due to perturbed plasma currents. With feedback current proportional to this net signal such that the feedback field at r = b is (-G) times this net signal,

$$\left(\left.\frac{\partial\psi}{\partial r}\right|_{r=b}\right)_{coil} = -G\left(\left.\frac{\partial\psi}{\partial r}\right|_{r=b}\right)_{plasma}.$$

This system is like a conducting wall with the image current enhanced by a factor G.

Using the relation between B_f and the coil's field at r = b, namely

$$\left(\left.\frac{\partial\psi}{\partial r}\right|_{r=b}\right)_{coil} = \left(\frac{b}{a}\right)^{m-1}(-iB_f),$$

we have the total field related to G by

$$\left(\left.\frac{\partial\psi}{\partial r}\right|_{r=b}\right)_{Total} = \left(1-\frac{1}{G}\right)\left(\frac{b}{a}\right)^{m-1}(-iB_f).$$

Using the general form for ψ (Eq. 4) to evaluate $\frac{\partial\psi}{\partial r}$ at r = b, we obtain the relation between B_{fo} and G as

$$B_{fo} = B_a \frac{\xi_a}{a} \left(\frac{(a/b)^{2m}}{1 - G\left(\frac{a}{b}\right)^{2m}} \right) (m-nq_a).$$

Using this expression for B_{fo} in our stability criterion (Eq. 15), we have

$$\left[-(m-nq_a) + \frac{(m-nq_a)^2}{1 - G\left(\frac{a}{b}\right)^{2m}} - (m-nq_a)^2 \frac{1}{2} \left(1 - \frac{a/m}{L_r}\right) \right] \geq 0. \tag{21}$$

Thus a gain G near but no greater than $(b/a)^{2m}$ greatly enhances the stabilizing first term. The requirement on G for stability is thus

$$\left(\frac{b}{a}\right)^{2m} \geq G \geq \left(\frac{b}{a}\right)^{2m} \left[1 - \{m-nq_a\} \Big/ \left\{ 1 - (m-nq_a) \frac{1}{2} \left(1 - \frac{a/m}{L_r}\right) \right\} \right].$$

The upper bound on G occurs because $G \geq \left(\frac{b}{a}\right)^{2m}$ reverses the sign of B_{fo}/ξ_{ao}.

i. Simple Feedback System and External Geometry Considerations

Another feedback system of interest is one that would simulate a wall very close to the plasma. For several reasons, a magnetic pickup loop could be positioned closer to the surface of the plasma than a wall could be. If the feedback current (which is flowing in coils at r = c) is driven so that the net radial flux measured by the probe at r = b is zero, then the stabilization would be the same as if a wall were located at r = b. This system has the boundary condition

$$\left.\frac{\partial\psi}{\partial r}\right|_{r=b} = 0$$

which gives

$$B_{fo} = B_a \frac{\xi_{ao}}{a} (m-nq_a) \frac{(a/b)^{2m}}{1 - (a/b)^{2m}} \tag{22}$$

and, just as for a wall at r = b (Eq. 20), the plasma is stabilized for some q_a values but is still unstable for q_a such that

$$0 < (m-nq_a) < \left[1 - \left(\frac{a}{b}\right)^{2m}\right] \left[\frac{1}{1 - \frac{1}{2}\left(1 - \left(\frac{a}{b}\right)^{2m}\right)\left(1 - \frac{a/m}{L_r}\right)} \right]. \tag{23}$$

The advantage of this system is that $1 - \left(\frac{a}{b}\right)^{2m}$ might be quite small, which would open a rather wide range of stable q_a values. (Note that the unstable range depends on L_r; but for this feedback scheme, B_{fo} and K_{fo} depend only on q_a.) Current requirements for this system are given below.

j. Relationship between B_f and K_f

Finally, we should state the relation of B_f to K_f, in order to give an indication of the currents needed for obtaining the required B_{fo} values. K_f and B_f are illustrated in Fig. VII-7, with

$$K_f = K_{fo} \exp(im\theta + ik_z z + \gamma t)$$

and K_f is related to B_f (for K_f flowing at $r = c$) by

$$B_f = \left(\frac{\mu_o}{2}\right) K_f \left(\frac{a}{c}\right)^{m-1}.$$

Thus, for the feedback system just considered, the K_{fo} needed to produce the B_{fo} in Eq. 22 is

$$K_{fo} = \frac{2}{\mu_o}\left[B_a \frac{\xi_{ao}}{a}(m-nq_a)\frac{(a/b)^{2m}}{1-(a/b)^{2m}}\right]\left(\frac{c}{a}\right)^{m-1}, \tag{24}$$

with K_{fo} in A/m.

This value for K_{fo} ignores the effects of other conductors. If there were a wall at $r = d$ (with $d > c$), then this wall would carry two image currents, one driven by K_f and the other by the perturbed plasma currents. The sum of the fields, because of the two image currents, plus K_f gives the net value of B_f. Although the ψ expression given previously (Eq. 4) is only valid out to the feedback coils, it is not too difficult to show that $\tilde{B}_{rf}$ for this geometry is given ($\tilde{B}_{rf}$ is defined as the radial field at $r = a$ that is due to all external currents and is related to B_f by $B_f = i\tilde{B}_{rf}$) by

$$\tilde{B}_{rf}\left[1-\left(\frac{a}{d}\right)^{2m}\right] = -i\frac{\mu_o}{2}K_f\left(\frac{a}{c}\right)^{m-1}\left[1-\left(\frac{c}{d}\right)^{2m}\right] - ik_{\parallel}B\xi_a\left(\frac{a}{d}\right)^{2m}$$

or

$$K_f = \frac{2}{\mu_o}\,\frac{(c/a)^{m-1}\left(1-\left(\frac{a}{d}\right)^{2m}\right)}{1-\left(\frac{c}{d}\right)^{2m}}\left[B_f - B_a\frac{\xi_{ao}}{a}(m-nq_a)\frac{(a/d)^{2m}}{1-\left(\frac{a}{d}\right)^{2m}}\right]. \tag{25}$$

This expression, relating K_f, B_f, and ξ_a, when K_f is at $r = c$ and a wall is at $r = d$, applies to any sensing arrangement.

Thus for the particular sensing arrangement just considered, where B_f is given by Eq. 22,

$$K_{fo} = \frac{2}{\mu_o}\left[B_a \frac{\xi_{ao}}{a}(m-nq_a)\,\frac{(a/b)^{2m}}{1-(a/b)^{2m}}\right]\left(\frac{c}{a}\right)^{m-1}\left[\frac{1-\left(\frac{b}{d}\right)^{2m}}{1-\left(\frac{c}{d}\right)^{2m}}\right]. \qquad (26)$$

This value for K_{fo} is much larger than the minimum K_{fo} required for stability, except near the marginally stable $m - nq_a$ value.

The minimum K_{fo} needed for stability can be found from the general stability relation (Eq. 15), since from Eq. 25 we know that the relation between B_{fo} and K_{fo} is

$$B_{fo} = \frac{\mu_o}{2} K_{fo}\left(\frac{a}{c}\right)^{m-1}\left(\frac{1-\left(\frac{c}{d}\right)^{2m}}{1-\left(\frac{a}{d}\right)^{2m}}\right) + B_a \frac{\xi_{ao}}{a}(m-nq_a)\,\frac{(a/d)^{2m}}{1-(a/d)^{2m}}. \qquad (27)$$

Substituting this expression in Eq. 15 gives the general stability requirement as

$$0 \leq (m-nq_a)^2\left[1 + \frac{a/m}{L_r} + \frac{2(a/d)^{2m}}{1-(a/d)^{2m}}\right] - 2(m-nq_a)\left[1 - \frac{K_{fo}\left(\frac{a}{c}\right)^{m-1}}{\bar{j}_{za}\xi_{ao}}\left(\frac{1-\left(\frac{c}{d}\right)^{2m}}{1-\left(\frac{a}{d}\right)^{2m}}\right)\right], \qquad (28)$$

where

$$\bar{j}_{za} \equiv \frac{2}{\mu_o}\left(\frac{B_a}{a}\right) = \bar{j}_z\Big|_{r=a}.$$

Thus the general stability criterion in terms of K_{fo} for this particular external geometry (but still applicable to any sensing arrangement) (for $m - nq_a$ positive) is

$$K_{fo} \geq \bar{j}_{za}\xi_{ao}\left(\frac{c}{a}\right)^{m-1}\frac{\left(1-\left(\frac{a}{d}\right)^{2m}\right)}{\left(1-\left(\frac{c}{d}\right)^{2m}\right)}\left[1 - \frac{m-nq_a}{2\left(1-\left(\frac{a}{d}\right)^{2m}\right)}\left\{2-\left(1-\frac{a^{2m}}{d^{2m}}\right)\left(1-\frac{a/m}{L_r}\right)\right\}\right] \qquad (29)$$

corresponding to the geometry-independent B_{fo} requirement in Eq. 16.

k. Conclusion

Using the energy principle, we have found the feedback field B_f needed (Eqs. 15, 16, and 18) to stabilize the MHD modes of a current-carrying plasma. This B_f requirement applies to any external coil and wall location and to any sensor-driver arrangement of the feedback system (that is, to any "boundary condition" imposed by a particular feedback scheme.)

The surfacelike feedback current K_f (units of A/m) needed to produce the required B_f depends on the external geometry. For the case of distributed feedback coils at $r = c$ and a conducting wall at $r = d$ $(d > c)$, the stability requirement in terms of K_f is given by Eq. 29.

Negative-Energy Kink Modes and Their Effect on the Requirement for the Feedback Stabilization of Kink Modes

a. Introduction

Linear feedback stabilization amounts to applying a B_f large enough that perturbations which are unstable without B_f, with B_f applied and exactly in phase with ξ_a, become stable propagating waves. If the plasma is rotating, it may be necessary to apply an extra B_f field to increase the propagation speed sufficiently to avoid the production of negative-energy modes.

The problem is that in a realistic system, the feedback field B_f is likely not to be exactly in phase with ξ_a but to lag slightly behind the propagating wave. In a plasma with no zero-order rotation, all of the stabilized modes have positive energy and the unstable modes have zero energy. Then a phase lag is no problem, since it merely causes some damping of the otherwise purely oscillatory modes. If the mode is a negative-energy mode, however, then such a phase lag causes growth. Even for very small phase lags this growth can be unacceptably large.

This phase-lag problem can be illustrated by considering conducting walls having resistivity η. For $\eta = 0$, a wave of amplitude ξ_a induces image currents that produce a feedback field B_f in phase with ξ_a. For finite η, the image currents lag behind the wave that drives them.

The consequences can be seen from energy conservation. The image current causes I^2R heating. By conservation of energy, as the wall gains energy, the wave must lose energy. If the wave energy is positive, then the wave amplitude must decrease. If the wave energy is negative, then the wave amplitude must increase (that is, the wave energy must become more negative) and so the wave grows in amplitude.

Thus a "lag" in B_f causes damping of positive-energy waves and growth of negative-energy waves. Likewise a "lead" turns out to cause a growth of positive-energy waves.

There are three ways to avoid wave growth caused by such lags or leads: (i) have no lags or leads in the feedback system; (ii) identify the type of wave and introduce lags for positive-energy waves and leads for negative-energy waves; or (iii) apply sufficiently large B_f that all stabilized waves are positive-energy waves and avoid leads by deliberately introducing a small lag, and hence introducing some damping of the stabilized wave. Only the third seems practicable; hence, we wish to show what is required to avoid negative-energy waves.

(i) Conservation of Action

Negative-energy modes occur only when the plasma has a zero-order rotation and the wave phase velocity relative to the plasma is slower than the rotational speed of the plasma. The waves have positive energy in the plasma frame but can have negative energy in the laboratory frame. The relation between wave energy and change of coordinate system introduces the concept of action conservation.

The energy of a wave depends on the velocity of the coordinate system in which the energy is measured. It is expected that the action, defined as the ratio of wave energy to wave frequency, will be an invariant with respect to change of inertial frames. The invariance of action corresponds to a conservation of wave quanta as for photons in vacuum where the observed energy in any coordinate system ($\hbar\omega_D$) divided by the observed frequency ω_D, the Doppler-shifted frequency, is a constant, $\hbar\omega_D/\omega_D$ or $\hbar$.

The kink modes can also be shown to be action-conserving. To show this, we consider what the wave energy is in nonrotating (with respect to the plasma) coordinates. By wave energy we mean the change in total energy of the whole system when the wave is present minus the total energy of that same system without the wave. In particular, the zero-order system energy may vary with coordinate system velocity. We consider only the case of a uniformly distributed current wherein the waves are essentially surface waves, and we take the displacement vector $\underline{\xi}(r,\theta,z)$ as having the spatial form that $\underline{\xi}$ has at marginal stability; that is, we take $\xi_z \approx 0$ and $\xi_\theta \approx i\xi_r$, with

$$\xi_r = \xi_a\left(\frac{r}{a}\right)^{m-1}.$$

This spatial dependence for $\underline{\xi}(r,\theta,z)$ applies to $\bar{j}_z$ = constant and $k_z^2 \ll \left(\frac{m}{r}\right)^2 (m-nq_a)$.

Thus the perturbed particle motion (for small k_z) is approximately a circulatory motion in the r-θ plane, with $\tilde{v}_r$ and $\tilde{v}_\theta$ varying with radius as $(r/a)^{m-1}$, where

$$\tilde{v}_r = \frac{\partial\xi_r}{\partial t} = \gamma\xi_r = -i\omega\xi_r$$

and

$$\tilde{v}_\theta = \frac{\partial \xi_\theta}{\partial t} = \gamma \xi_\theta = -i\omega \xi_\theta.$$

Here, γ is the growth rate (or $\omega = i\gamma$ is the frequency) in the ξ_r expression

$$\xi_r = \xi_{ao}\left(\frac{r}{a}\right)^{m-1} \exp(im\theta + ik_z z + \gamma t).$$

If the plasma is at rest in the coordinate system so that there is no zero-order directed velocity, then the perturbed kinetic energy δK is

$$\delta K = \int d\tau\, \frac{\gamma\gamma^*}{2}\, \rho\left(\xi_r^2 + \xi_\theta^2 + \xi_z^2\right), \tag{30}$$

where $d\tau$ denotes volume integration, and ρ is the mass density. For illustrative purposes, ρ is taken to be independent of radius (the pressure gradient is taken up by a temperature gradient). Thus, with the dz integration taken over $2\pi R$, and $\xi_r^2 + \xi_\theta^2 + \xi_z^2$ being $\xi_{ao}^2\left(\frac{r}{a}\right)^{2m-2}$ and independent of θ and z, we obtain

$$\delta K = 2\pi R \int_0^a dr\, (2\pi r)\, \frac{\rho}{2}\, \gamma\gamma^* \xi_{ao}^2 (r/a)^{2m-2}$$

$$= 2\pi R\, \frac{\pi a^2}{2m}\, \rho \xi_{ao}^2 \gamma\gamma^* = W_o\left(\mu_o \rho a^2/B_a^2\right) \gamma\gamma^*.$$

Together with this wave kinetic energy, there is the wave potential energy δW, which for $(r\xi_r)'/(r\xi_r) = \frac{m}{r}$ is

$$\delta W = W_o \beta, \tag{31}$$

where

$$W_o = 2\pi R(\pi a^2)\, B_a^2/2\mu_o\left(\frac{1}{m}\, \xi_{ao}^2/a^2\right),$$

and

$$\beta = \left[2(m-nq_a)^2 - 2(m-nq_a) + 2(m-nq_a)\, \frac{B_f}{B_a(\xi_a/a)}\right]. \tag{32}$$

For unstable waves the total wave energy $\delta W + \delta K$ must be zero, since the wave grows or damps without any energy being added or subtracted by an external source. For growing (or damping) waves $\gamma\gamma^*$ is just γ_r^2, γ_r = real part of γ. Thus, with

$$\delta K = W_o\left(\mu_o \rho a^2/B_a^2\right) \gamma_r^2 \tag{33}$$

and

$$\delta W = W_o \beta,$$

we have $(\delta K + \delta W = 0)$, which implies

$$W_o\left(\frac{\mu_o \rho a^2}{B_a^2}\right) \gamma_r^2 = -W_o \beta.$$

This, with no feedback $(B_f = 0)$, means that growing waves can occur for q_a values such that $0 < m - nq_a < 1$.

For stable waves, $\gamma\gamma^*$ is ω^2 and δK is still positive. δW is also positive and equal to δK. That is,

$$W_o\left(\frac{\mu_o \rho a^2}{B_a^2}\right) \omega^2 = W_o \beta.$$

Thus the total wave energy U_T for a propagating mode is

$$U_T = \delta W + \delta K = 2W_o \beta. \tag{35}$$

These wave energies are for the coordinate frame moving with the plasma.

(ii) Wave Energy in a Rotating Frame

Now consider a coordinate system rotating with angular velocity $\partial\theta/\partial t$ or velocity v_θ,

$$v_\theta = r \frac{\partial\theta}{\partial t} = \left(\frac{r}{a}\right) v_{\theta a}.$$

As viewed from this coordinate system, the plasma has a zero-order rotational velocity of $(-v_\theta)$. Also, if ω_o denotes the wave frequency measured in nonrotating coordinates, then the frequency in the rotating coordinate system ω is given by

$$\omega = \omega_o - \frac{m}{r} v_\theta = \omega_o - \frac{m}{a} v_{\theta a}.$$

Besides the frequency shift caused by change of coordinate system, there is a new contribution to the wave energy. In the new coordinate system, the plasma has a finite zero-order azimuthal rotational velocity $(-v_\theta)$. This zero-order velocity, when dotted into the perturbed velocity times ρ, contributes an additional kinetic piece to the wave energy. This new contribution, which we denote δK_R, represents the increase or decrease in the energy stored in zero-order rotational kinetic energy. When this decrease in rotational energy is larger than $\delta W + \delta K$, the wave energy is negative. δK_R is the volume integral of $\rho(-v_\theta) \frac{\partial \xi_\theta}{\partial t}$ and is second-order in the wave amplitude; $\rho(-v_\theta) \frac{\partial \xi_\theta}{\partial t}$ is first-order, but it goes as $\cos m\theta$ and the average over θ gives zero everywhere, except in the region between $r = a - \xi_{ao}$ and $r = a + \xi_{ao} \cos m\theta$. Thus the fraction of the volume making a net contribution to δK_R is first-order in ξ_{ao}/a, which makes δK_R second-order in (ξ_{ao}/a).

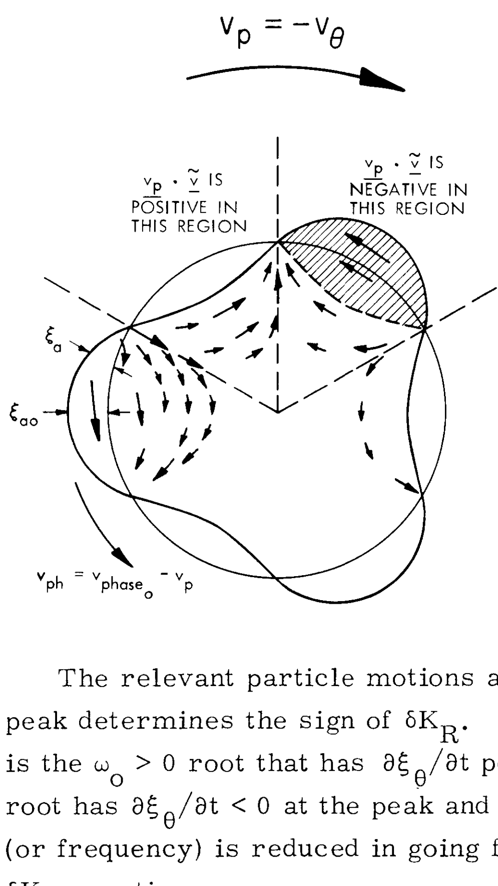

Fig. VII-8.

Particle motions for a stable wave. Illustrating the change in wave energy for coordinate system velocity v_θ, or correspondingly plasma rotational velocity v_p. Particle motions are for a wave with positive $(+\theta)$ phase velocity relative to the plasma. Shaded region gives the net contribution to δK_R.

The relevant particle motions are shown in Fig. VII-8. The direction of $\partial\xi_\theta/\partial t$ at the peak determines the sign of δK_R. Of the two stable roots of the dispersion relation, it is the $\omega_o > 0$ root that has $\partial\xi_\theta/\partial t$ positive at the peak and negative δK_R, while the $\omega_o < 0$ root has $\partial\xi_\theta/\partial t < 0$ at the peak and positive δK_R. Thus the mode whose phase velocity (or frequency) is reduced in going from plasma coordinates to rotating coordinates has δK_R negative.

Now, to compute δK_R, we have

$$\delta K_R = \int d\tau \; \rho(-v_\theta) \frac{\partial \xi_\theta}{\partial t}$$

or, since the integral over $r = 0$ to $r = (a - \xi_{ao})$ gives zero,

$$\delta K_R = 2\pi R \int_0^{2\pi} a\, d\theta \int_{r=a-\xi_{ao}}^{r=a+\xi_{ao} \cos m\theta} dr \left\{ -v_\theta \frac{\partial \xi_\theta}{\partial t} \rho \right\}.$$

Now $\partial\xi_\theta/\partial t$ is related to ω_o and ξ_{ao} by $\xi_a = -i\xi_\theta \big|_{r=a}$ and by

$$\left.\frac{\partial \xi_\theta}{\partial t}\right|_{r=a} = -i\omega_o \xi_\theta \Big|_{r=a} = \omega_o \xi_{ao} \cos m\theta.$$

Thus

$$\delta K_R = 2\pi R \int_0^{2\pi} a\, d\theta \left[\rho(-v_{\theta a})(\omega_o \xi_{ao} \cos m\theta)\right]\left[\xi_{ao}(1 + \cos m\theta)\right]$$

$$= -W_o\left(\rho\mu_o a^2/B_a^2\right) 2 \frac{m}{a} v_{\theta a}\omega_o. \tag{36}$$

Noting that the frequency is $\omega = \omega_o - \frac{m}{a} v_{\theta a}$, and

$$\delta K = W_o\left(\rho\mu_o a^2/B_a^2\right) \omega_o^2,$$

we have

$$\delta K_R = -2(\delta K)\left[\frac{\omega_o - \omega}{\omega_o}\right]$$

or, since $\delta K = \delta W$ for propagating modes,

$$\delta K_R = -2\delta W\left[\frac{\omega_o - \omega}{\omega_o}\right]. \tag{37}$$

(iii) Total Wave Energy and Conservation of Action

Thus the total wave energy U_T is

$$U_T = \delta K_R + (\delta K + \delta W)$$

$$= \delta K_R + 2\delta W$$

$$= \frac{\omega}{\omega_o}(2\delta W) = \frac{\omega}{\omega_o} U_{To}, \tag{38}$$

where U_{TO} is $\delta K + \delta W$, the total energy as measured in the plasma frame. So, finally, we have the conservation-of-action result,

$$\frac{U_T}{\omega} = \frac{U_{To}}{\omega_o} \quad \text{or} \quad \frac{U_T}{\omega} = \text{constant.} \tag{39}$$

Thus the ratio of the measured energy to the measured frequency does not depend on the rotational speed of the coordinates in which the measurements are made.

b. Negative-Energy Waves

An alternative form for the total wave energy is

$$U_T = \frac{v_{ph}}{v_{ph_o}} U_{To}, \tag{40}$$

where v_{ph} and v_{ph_o} are the phase velocities as measured in the rotating frame and in the plasma frame, respectively. So if v_{ph}/v_{ph_o} is negative, then U_T is negative. Thus negative-energy waves occur when the plasma rotation is faster than v_{ph_o}, and hence the direction of the phase velocity is reversed. Now stable waves come in pairs with phase velocities (relative to the plasma) in opposite directions. With $|v_{\theta a}|$ larger than $|v_{ph_o}|$ both modes have v_{ph} in the same direction, and one mode can be termed the "slow wave" and the other the "fast wave." The "slow wave" is a negative-energy wave.

c. Conservation of Action for Unstable Modes

The unstable modes have δK positive and δW negative, with δK equal to $(-\delta W)$. Thus the total wave energy in the plasma frame is $U_{To} = \delta W + \delta K = 0$. When the problem is examined in rotating coordinates, there is again a new term δK_R because of the perturbed velocity dotted into the zero-order velocity, but $\partial\xi_\theta/\partial t$ now goes as $\sin m\theta$. Thus, the δK_R integration outside $r = (a-\xi_{ao})$ is a $d\theta$ integration over $\sin m\theta \cos m\theta$, rather than $\cos^2 m\theta$, and gives zero. With δK_R zero, U_T is still zero in rotating coordinate systems; hence, action conservation holds.

d. Growth of Negative-Energy Modes Because of Finite-Conductivity Walls

We have mentioned that resistive phase lags cause growth of negative-energy modes. We can compute the growth rate from the wall heating and conservation of energy. We now consider that the plasma actually has a zero rotation in the laboratory frame, say, induced by a zero-order radial electric field.

The image current $K_{f\ wall}$ flowing in a conducting wall at r = b is

$$K_{f\ wall} = K_{f\ wall_o} \exp(im\theta + ik_z - i\omega t) \approx K_{f\ wall_o} \cos m\theta\ e^{-i\omega t},$$

as shown in Fig. VII-7, and the magnitude that makes $\tilde{B}_r\big|_{r=b}$ zero is

$$K_{f\ wall_o} = \frac{2}{\mu_o} B_a \frac{\xi_a}{a} (m-nq_a)\left(\frac{a}{b}\right)^{m+1} \Bigg/ \left(1-\left(\frac{a}{b}\right)^{2m}\right). \tag{41}$$

For a wall with small but finite resistivity η, the current has essentially the same magnitude and can be taken to be flowing within a skin depth Δ of the wall surface at r = b. Thus dH/dt, the wall heating rate for a section of wall, $2\pi R$ long, is

$$\frac{dH}{dt} = 2\pi R \int_0^{2\pi} b\, d\theta\ \eta \left(\frac{K_{f\ wall_o} \cos m\theta}{\Delta}\right)^2 \Delta$$

or

$$\frac{dH}{dt} = 2\pi R\left(\frac{2\pi b}{2}\right)\left(\frac{\eta}{\Delta}\right) K^2_{f\ wall_o}. \tag{42}$$

Conservation of energy demands

$$\frac{dH}{dt} + \frac{d}{dt}(U_T) = 0, \tag{43}$$

where U_T is the total wave energy in the wall frame, and is related by conservation of action to U_{To}, the total wave energy in the plasma frame. If the centrifugal force corrections are negligible, U_{To} will still be $\delta K + \delta W = \delta W$, with $\delta W = W_o\, \beta_{wall}$, where, for small η, in order that the in-phase component of B_f will be as in Eq. 33,

$$\beta_{wall} \approx \beta_{wall,\ \eta=0} = 2\left[(m-nq_a)^2/(1-a^{2m}/b^{2m}) - (m-nq_a)\right]. \tag{44}$$

Thus U_T is related to β_{wall} by

$$U_T = \frac{\omega}{\omega_o} U_{To} = \frac{\omega}{\omega_o} 2W_o\beta_{wall}$$

$$= -\left(\frac{v_{\theta a}}{v_{ph}} - 1\right) 2W_o\beta_{wall}. \tag{45}$$

Combining these relations, we obtain γ_H, defined by

$$2\gamma_H = \frac{1}{U_T}\frac{dU_T}{dt}$$

or

$$2\gamma_H = \frac{1}{(-U_T)}\frac{dH}{dt}$$

which is positive if $v_{\theta a} > \frac{\omega_o}{m/a}$, so that U_T is negative.

Using the values for dH/dt from Eq. 42 and for U_T from Eq. 45, we obtain

$$\gamma_H = \frac{1}{2\beta_{\substack{wall\\ \eta=0}}}\left[\frac{\eta}{\Delta}\left(\frac{m/b}{\mu_o}\right)\frac{4(a/b)^{2m}}{(1-(a/b)^{2m})^2}\right]\left[\frac{v_{\theta a}}{v_{ph_o}} - 1\right]. \tag{46}$$

This result for γ_H agrees with Rutherford and Furth's resistive-wall report,[5] in which they refer to these resistively growing negative-energy modes as pseudo kinks.

For a nonrotating plasma ($v_{\theta a} = 0$), γ_H is negative and the waves damp as expected. The damping rate is rather rapid for Tokamak-like conditions, especially for small β_{wall}. For copper, $\frac{\eta}{\Delta} \approx 10^{-4}\ \Omega$ at 10^5 Hz and that gives

$$\gamma_H \approx 10^3\left[\frac{m(a/b)^{2m}}{(1-(a/b)^{2m})^2\ \beta_{wall}}\right]\left[\frac{v_{\theta a}}{v_{ph_o}} - 1\right].$$

The quantity in brackets is of order one for low m-number modes that are not too far from the unstable range for $m - nq_a$ $\left(\text{zero to } 1 - \frac{a^{2m}}{b^{2m}}\right)$, which gives a damping time of the order of a millisecond for no rotation (or for $v_{\theta a} \ll v_{ph_o}$). Likewise, if $v_{\theta a}$ is twice v_{ph_o}, then the growth rate may be of the order of a millisecond.

Aside from the necessity to conserve energy, the resistive wall effects can also be thought of as resulting from the phase lag of B_f behind the wave. Consider the case in which $v_{\theta a}$ is zero and the waves are damped by the resistivity. As the wave propagates along the wall, the image current $K_{f\,wall}$ in the wall lags behind the boundary displacement ξ_a by an "R/ωL" phase lag. By computing the magnetic energy produced by $K_{f\,wall}$, the inductance "L" can be computed, and the "R" is related to the ratio of resistivity to skin depth, (η/Δ). (Δ is related to η and to the frequency, but it is much clearer to leave the results in terms of Δ.) The phase lag "R/ωL" or $m(\Delta\theta)$ is found to be

$$m(\Delta\theta) = \frac{1}{\omega}\left[\frac{\eta}{\Delta}\left(\frac{m/b}{\mu_o}\right)\frac{2}{1-\left(\frac{a}{b}\right)^{2m}}\right]. \tag{47}$$

Thus B_f, the azimuthal component at r = a of the magnetic field produced by K_f is

$$B_f = B_{f,\,\eta=0}\left[1 - \frac{i}{\omega}\left(\frac{\eta}{\Delta}\right)\frac{m/b}{\mu_o}\left(\frac{2}{1-\left(\frac{a}{b}\right)^{2m}}\right)\right], \tag{48}$$

under the assumption that for small η the component of B_f in phase with ξ_a is still $B_{f,\,\eta=0}$ (Eq. 19).

We now obtain the damping rate by using this B_f in the dispersion relation

$$\delta K = W_o\left(\frac{\rho\mu_o a^2}{B_a^2}\right)\omega^2 = \delta W = W_o\beta,$$

where

$$\beta = 2(m-nq_a)^2 - 2(m-nq_a) - 2(m-nq_a)\frac{B_f/\xi_a}{B_a/a},$$

with B_f, now complex, given by Eq. 48. With β complex, when the real part of β is positive and the waves are propagating waves of frequency ω, ω has a small imaginary part, a growth rate γ_H, which can easily be solved for in the approximation that the real part of ω is essentially the same as for $\eta = 0$ (that is, we take the real part of β to be $\beta_{\substack{\text{wall}\\ \eta=0}}$). The result is

$$\gamma_H = -\frac{1}{2\beta_{\substack{\text{wall}\\ \eta=0}}}\frac{\eta}{\Delta}\left(\frac{m/b}{\mu_o}\right)\frac{4(a/b)^{2m}}{[1-(a/b)^{2m}]^2},$$

as we found for $v_{\theta a} = 0$ (Eq. 46).

Similar conclusions about damping or growth can be reached by examining the electric field arising from the time rate of change of B_f.

e. Need for Extra B_f to Avoid Forming Negative-Energy Modes

We are led to the conclusion that unavoidable (perhaps desirable) phase lags in B_f will cause non-negligible growth of negative-energy modes. Thus we want all stabilized modes to be positive-energy modes, which requires that the part of B_f in phase with ξ_a be large enough that the stabilized mode's phase velocity relative to the plasma be larger than the rotational velocity of the plasma.

The phase velocity relative to the plasma depends on δW, with δW depending on B_f. Since $\delta W = \delta K$ for propagating modes and δK is related to the phase velocity relative to the plasma by Eq. 16, we see that B_f must be such that δW (or δK) is greater than $\delta K \big|_{\omega_o = \frac{m}{a} v_{\theta a}}$, the δK value for a wave having v_{ph_o} equal to $v_{\theta a}$. That is, we require

$$\delta W \geqslant \left(\delta K \Big|_{\omega_o = \frac{mv_{\theta a}}{a}} \right) = W_o \left(\frac{\mu_o \rho a^2}{B_a^2} \right) \left(\frac{m}{a} v_{\theta a} \right)^2 = W_o m^2 \left(\frac{v_{\theta a}^2}{B_a^2/\rho\mu_o} \right).$$

For such δW, $|v_{ph_o}| > |v_{\theta a}|$ and no negative-energy waves can occur.

In terms of β, where $\delta W = W_o \beta$, and β depends upon B_f, as given by

$$\beta = 2(m-nq_a)^2 - 2(m-nq_a) + 2(m-nq_a) \frac{B_f/\xi_a}{B_a/a},$$

all stabilized modes will have positive wave energy if β_r, the real part of β, is

$$\beta_r \geqslant m^2 \left(\frac{v_{\theta a}^2}{B_a^2/\rho\mu_o} \right).$$

f. Changes in Stability Requirements because of Finite Wall Resistivity or the Necessity of Avoiding the Presence of Negative-Energy Modes

The β requirement described above demands a larger B_f than is needed for the stability requirement $\beta \geqslant 0$, as is appropriate for nonrotating plasma.

The origins of the increase in feedback requirements are qualitatively interesting, but quantitatively small, for likely rotational speeds in Tokamak-type devices. For example, a radial electric field of the order of KT_i/ea is reasonable, and for the extra β needed gives

$$\frac{v_{\theta a}^2}{B_a^2/\rho\mu_o} = \left[\frac{nKT_i}{B_a^2/\mu_o} \right] \left[\frac{m_i v_i/eB_z}{a} \right]^2,$$

where KT_i/e is the ion temperature in volts, m_i is the ion mass, and v_i is the ion thermal velocity. The first bracketed quantity is the poloidal beta which is likely to be around unity, while the second bracketed quantity is the ratio of the ion gyro radius to the plasma radius squared, which is small.

Also small is the correction to the usual range of unstable q_a values for kink modes partially stabilized by a conducting wall at $r = b$. For a perfectly conducting wall the stability criterion (for constant current density) is

$$\beta_{wall} = 2 \frac{(m-nq_a)^2}{1-(a/b)^{2m}} - 2(m-nq_a) > 0,$$

or the plasma is unstable for q_a so that

$$0 < (m-nq_a) < 1 - \left(\frac{a}{b}\right)^{2m}.$$

If the plasma is rotating, half of the barely stabilized waves (the "slow waves") will be negative-energy waves. Thus for finite η, we need q_a values such that

$$\beta_{wall} \geq m^2 \frac{v_{\theta a}^2}{B_a^2/\rho\mu_o},$$

in order to avoid the production of negative-energy kink modes, which would grow for any finite wall resistivity. Thus the $(m-nq_a)$ range for which the plasma is unstable is widened to

$$-\frac{m^2}{2} \frac{v_{\theta a}^2}{B_a^2/\rho\mu_o} < (m-nq_a) < \left[1 - \left(\frac{a}{b}\right)^{2m} + \frac{m^2}{2} \frac{v_{\theta a}^2}{B_a^2/\rho\mu_o}\right], \tag{50}$$

but again the correction is small.

R. S. Lowder, K. I. Thomassen

References

1. I. Bernstein, E. A. Frieman, M. D. Kruskal, R. Kulsrud, Proc. Roy. Soc. (London) A244, 17-40 (1958).
2. R. S. Lowder and K. I. Thomassen, Quarterly Progress Report No. 104, Research Laboratory of Electronics, M. I. T., January 15, 1972, pp. 172-184.
3. W. A. Newcomb, Ann. Phys. (N.Y.) 10, 232 (1960).
4. V. V. Arsenin and V. A. Chuyanov, Soviet Atomic Energy 25, 902-903 (1968).
5. P. H. Rutherford and H. P. Furth, MATT-872 (December 1971), Plasma Physics Laboratory, Princeton University, Princeton, New Jersey and internal report.

VII. PLASMAS AND CONTROLLED NUCLEAR FUSION*

F. High-Temperature Plasma Physics

Academic and Research Staff

Prof. B. Coppi
Dr. D. B. Montgomery†
Prof. G. Bekefi
Prof. A. Bers
Prof. R. A. Blanken
Prof. R. J. Briggs
Prof. L. M. Lidsky
Prof. R. R. Parker
Prof. K. I. Thomassen
Dr. E. Minardi
Dr. L. Ornstein
Dr. P. A. Politzer
Dr. J. Rem
Dr. D. Schram
Dr. F. C. Schüller
Dr. D. J. Sigmar
A. Hugenholtz

Graduate Students

E. L. Bernstein
D. L. Cook
D. P. Hutchinson
Y. Y. Lau
M. A. Lecomte
A. R. Millner
T. Orzechowski
N. R. Sauthoff
M. Simonutti
B. V. Waddell
D. C. Watson
S. M. Wolfe

1. RESONANT SCATTERING OF TRAPPED PARTICLES BY TOROIDAL PLASMA MODES

In two-dimensional plasma configurations electrostatic modes are shown to be excited with frequency and parity characteristics such as to affect significantly the orbits ("quasi bananas") of trapped ions by proper mode-particle resonances. Processes of this kind, in fact, may provide an effective scattering mechanism in regimes where the single-particle collision mean-free paths are considerably longer than the periodic particle excursions.

It is expected that in magnetically confined plasmas wherein the collisional mean-free paths are much longer than the periodicity length of the lines of force, the major transport parameters will be only partially accounted for by the effects of single-particle collisions.[1] An aspect of this circumstance is the observed absence of current skin layers in diffuse-pinch experiments, which is contrary to what would be expected when considering only the effects of collisions on the plasma electrical resistivity and electron thermal conductivity. A related question is whether trapped particles, in a toroidal magnetic configuration, can be lost by large-scale instabilities in the high-temperature regimes where the effects of collisional scattering become negligible, as indicated by the theoretical analysis. The fraction of trapped particles is, in fact, more than half of the total population in most of the diffuse-pinch experiments now being realized.

*This work was supported by the U.S. Atomic Energy Commission (Contract AT(11-1)-3070).

†Dr. D. Bruce Montgomery is at the Francis Bitter National Magnet Laboratory.

We find that collective modes capable of causing resonant scattering of trapped ions, in fact, can be excited, under realistic conditions on the ion temperature and density gradients, in two-dimensional plasma confinement configurations. A significant asymptotic limit also exists in which the influence of the excited modes on the trapped-particle orbits can be evaluated analytically.

We represent the toroidal magnetic field by $B_\zeta = B_o[1+(r/R_o)\cos\theta]^{-1}$, where r is the magnetic surface, and θ and ζ are the poloidal and toroidal angles, respectively. An important class of modes that can be excited, in the limit where $8\pi nkT \ll B_o^2$, is electrostatic ($\underline{E}_1 = -\nabla\tilde{\Phi}$). Since the equilibrium configuration is nonhomogeneous in θ, the normal-mode solutions for $\tilde{\Phi}$ of the linearized plasma equations are of the form $\Phi = \tilde{\phi}_{m^o,n^o}(r,\theta)\exp(-i\omega t + im^o\theta - in^o\zeta)$, where m^o and n^o are integers. We indicate by χ the rationalized rotational transform ($\chi \approx R_oB_\theta/(rB_\zeta)$), and, in particular, consider modes that are localized in the radial direction around a rational surface $r = r_o$ such that $\chi(r_o) = n^o/m^o$. The electric field $\tilde{E}_\parallel = \vec{E}_1 \cdot \vec{B}/B$ associated with these modes is $\tilde{E}_\parallel \approx -(1/r_o)(\partial/\partial\theta)\,\tilde{\phi}_m(\theta)$, where we define $\tilde{\phi}_m(\theta) \equiv \tilde{\phi}_{m^o,n^o}(r_o,\theta)$. Therefore the θ dependence of $\tilde{\phi}_m$ is an important feature in determining the resonant interaction between particles and excited modes. Notice that the magnetic field $B \approx B_\zeta$ is minimum about $\theta = 0$. Then, with reference to this point, the modes under consideration can be distinguished as odd and even.[2] The corresponding field $\tilde{E}_\parallel$ is even and odd about $\theta = 0$. We shall not consider flute modes for which $(\partial\tilde{\phi}_m/\partial\theta)/\tilde{\phi}_m$, and therefore $\tilde{E}_\parallel$ is insignificant. Consequently, all modes of interest propagate along the toroidal (ζ) direction with phase velocity $v_{ph} = \omega R/n^o$.

It is clear, then, that odd modes tend to affect the dynamics of deeply trapped particles more than even modes. For this reason, we made a survey of the modes that can be excited in a typical diffuse-pinch experiment and found that their frequency of oscillation ω is likely to be closer to the ion average bounce frequency, $\langle\omega_b\rangle_i$, than to that of the electron. Therefore we were led to consider resonant scattering of trapped ions, and to focus attention on modes that are not heavily damped by wave-particle resonances when $\omega \approx \langle\omega_b\rangle_i$. Such modes can be visualized as a kind of negative energy waves,[3] in a proper frame of reference, whose instability can be associated with dissipative effects or Landau dampings in collisionless plasmas.

The modes that most closely fulfill these requirements are driven by the ion temperature gradient. The stability properties of these modes in the two-dimensional equilibrium configuration that we are considering are substantially different from those that are found in a one-dimensional configuration. It has been suggested that ion temperature-driven modes play an important role in determining the ion thermal-energy transport across the magnetic field in Tokamak experiments.[4] We analyze the limit $\omega < \langle\omega_b\rangle_i < \langle\omega_b\rangle_e$ and decompose $\tilde{\phi}_m(\theta)$ in harmonics of the orbit periodicity

$\tilde{\phi}_m = \Sigma\, \tilde{\Phi}_m^{(p)}(\lambda) \exp[i2p\omega_b \hat{t}]$, where $\hat{t} = R \int^{\theta} d\theta'/(v_{\|}\chi)$, $\lambda = \epsilon/\mu$, $\epsilon = \frac{1}{2} m\left(v_{\perp}^2 + v_{\|}^2\right)$ is the particle kinetic energy, $\mu = \frac{1}{2} mv_{\perp}^2/B$ is the magnetic moment, $\omega_b = 2\pi/\tau$, $\tau = R \oint d\theta/(v_{\|}\chi)$ for trapped particles, and $\tau = R \int_0^{4\pi} d\theta/(v_{\|}\chi)$ for circulating particles.[1] For circulating particles, ω_b has the sign of $v_{\|}$. In particular, for odd modes the average potential over a particle orbit $\Phi_m^{(o)} = \tau^{-1} R \oint d\theta\, \phi_m(\theta)/(\chi v_{\|}) = 0$. Therefore[2] the perturbed electron density is simply $\tilde{n}_e = en\tilde{\phi}/T_e$. Notice that, since $\tilde{n}_e$ and $\tilde{\phi}$ are in phase, no particle loss is caused by these modes. The assumed ion equilibrium distribution is of the form $f_i = f_{Mi}(1+\hat{f}_i)$, $\hat{f}_i = -(v_{\|}/\Omega_{\theta i})[(dn_i/dr)/n_i - (dT_i/dr)(3/2-\epsilon/T_i)/T_i]$, $\Omega_{\theta i} = eB_{\theta}/(m_i c)$, and f_{Mi} is the Maxwellian. The expression for $\tilde{n}_i$ is then obtained by integrating the Vlasov equation along particle orbits in the zero Larmor radius limit.

$$\tilde{n}_i = -(en/T_i)\left\{\tilde{\phi}_m - n^{-1} \int d^3\vec{v}\, f_{oi}\left[\omega - \omega_{*i} + \omega_{T_i}(3/2 - \epsilon/T_i)\right] \cdot \sum_p \left[\tilde{\Phi}_m^{(p)}(\lambda) \exp(i2p\omega_b \hat{t})\right]/(\omega - 2p\omega_b)\right\}, \tag{1}$$

where $\omega_{*i} = -(m^o/r)(dn/dr)cT_i/(eBn)$, and $\omega_{T_i} = \omega_{*i}(d\ln T_i/dr)/(d\ln n/dr)$. Then we consider the quadratic form which results from the quasi-neutrality condition expressed as $\oint d\ell\, \tilde{\phi}_m{}^* (\tilde{n}_i - \tilde{n}_e)/B = 0$, where $d\ell = R\, d\theta/\chi$,

$$(1+T_i/T_e)\; n \oint d\ell\, |\tilde{\phi}_m|^2/B - (\pi/2)(2/m_i)^2 \iint d\epsilon d\mu\, f_{Mi} |2\pi/\omega_b| \cdot \left[\omega - \omega_{*i} + \omega_{T_i}\left(\frac{3}{2} - \epsilon/T_i\right)\right] \sum_{p\neq 0} \left[|\tilde{\Phi}_m^{(p)}(\lambda)|^2/(\omega - 2p\omega_b)\right].$$

In the limit $\omega < \langle \omega_b \rangle_i < \omega_{T_i} \sim \omega_{*i}$ we obtain

$$(1+T_i/T_e) \oint d\ell\, |\tilde{\phi}_m|^2/B + \left(\omega_{*i} - \omega_{T_i}\right)\omega/(4\pi^2) \int d\lambda \left(L_o^3(\lambda)/v_{thi}^2\right) \sum_{p\neq 0} |\tilde{\Phi}_m^{(p)}(\lambda)|^2/p^2$$

$$- i\omega^2\left(3\omega_{T_i}/2 - \omega_{*i}\right)/(8\pi^{5/2}) \int d\lambda \left(L_o^4(\lambda)/v_{thi}^3\right) \sum_{p\neq 0} |\tilde{\Phi}^{(p)}(\lambda)|^2/|p|^3 = 0, \tag{2}$$

where $2L_o(\lambda) = \oint d\ell/(1-\lambda B)^{1/2}$, and $v_{thi} = (2T_i/m_i)^{1/2}$. This equation shows that instability occurs for

$$\frac{1}{T_i}\frac{dT_i}{dr} > \frac{2}{3}\frac{1}{n}\frac{dn}{dr}. \tag{3}$$

We recall that in a one-dimensional configuration,[5] instability can be found only if $d \ln T_i/dr > d \ln n/dr$ and by considering very short wavelengths, of the order of the ion gyro radius.[6] For the present case, the frequency ω can no longer be considered smaller than $\langle \omega_b \rangle_i$, and the expansion leading to Eq. 2 is not valid in the limit when $d \ln T_i/dr$ tends to equal $d \ln n/dr$. The difference between the nature of the dispersion relation for a one-dimensional geometry, as given, for instance, by Galeev et al.,[5] and the one presented here arises because in the former case Landau resonances $\omega = k_{\parallel}v_{\parallel}$ are involved, with no constraint on the value of $v_{\perp}$ ($k_{\parallel}$ is the wave number in the direction of $\vec{B}$). In our case the relevant resonances are of the form $\omega = \omega_b(\epsilon, \mu)$ and involve a considerably smaller portion of velocity space[2] (in practice, surfaces of constant ϵ). The instability criterion (3) would have been slightly modified had we considered a collision-dominated equilibrium[7] in which the expression for $\hat{f}_i$ relevant to circulating particles is different from the one assumed here.

The particle equation of motion in θ under the influence of the fluctuating electric field can be derived from

$$(d\epsilon/dt) = -e\vec{v} \cdot \nabla\tilde{\Phi} = -e(d\tilde{\Phi}/dt - \partial\tilde{\Phi}/\partial t),$$

where $v_{\parallel} = (d/dt)(R\theta(t)/\chi)$. Neglecting the magnetic curvature drift, as allowed by a realistic choice of parameters, we then have

$$(d^2\theta/dt^2) + \omega_{ob}^2 \sin\theta = -(e/m)(\chi/R)^2 (d\theta/dt)^{-1} (d\tilde{\Phi}/dt - \partial\tilde{\Phi}/\partial t)$$

$$= \omega_{ob}^2(\hat{\alpha}/\tilde{\phi}_c)(d\tilde{\phi}_m(\theta)/d\theta) \cos(\omega t), \tag{4}$$

where $\omega_{ob}^2 = \left(\mu B_o \chi_o^2\right)/\left(mR_o^2\right)(r/R_o)$ represents the bounce frequency of trapped particles with amplitudes $\theta < (6)^{1/2}$, $\tilde{\phi}_c$ is a typical amplitude of the fluctuating potential, and $\hat{\alpha} = e\tilde{\phi}_c R/(\mu B_o r)$. We consider the case of deeply trapped particles with excursion amplitudes such that $(d/d\theta)\tilde{\phi}_m \approx (\tilde{\phi}_c/\theta_{od}) \cdot \left(1 + \alpha_2\theta^2 + \alpha_4\theta^4 + \dots\right)$ over them. Then, for $\alpha_2\theta^2 < 1$, Eq. 4 becomes

$$\ddot{\theta} + \theta - \theta^3/6 = \alpha \cos \omega_o t_o, \tag{5}$$

where $t_o = t\omega_{ob}$, $\omega_o = \omega/\omega_{ob}$ and $\alpha = (\hat{\alpha}/\theta_{od}) \sim (e\tilde{\phi}_c/T_i)(R_o/r\theta_{od})$, since we refer to resonances with trapped ions. Note, for instance, that if $e\tilde{\phi}_c/T_e \approx 2 \times 10^{-2}$, $R_o/(r\theta_{od}) \sim 6$, and $T_e \sim 2T_i$, the parameter α is not a really small number. The solution of Eq. 5 can be written[7] in the form $\theta = 2\chi(t_o) \cos [\omega_o t_o - \psi(t_o)]$, where the amplitude $\chi(t_o)$ satisfies

$$\chi^4/4 + 2\chi^2(\omega_o - 1) + a\chi \cos \psi = c. \tag{6}$$

The constant c is determined by the initial conditions, and the phase ψ is given by $d\psi/dt_o = (1/4)\chi^2 + (\omega_o - 1) + (a/4\chi) \cos \psi$. The limit $a = 0$, where $\psi = (\omega_o - 1)t_o$ and χ = const, corresponds to the unperturbed "banana" orbit in the torus. In the same limit, if we introduce Van der Pol coordinates $a = 2\chi \cos \psi$ and $b = 2\chi \sin \psi$, these orbits correspond to circles centered about O. The amplitude of the oscillation is represented by the polar vector rotating in time around O. We recall that trapped particles correspond to a pitch angle range $-r/R_o < \Lambda - 1 < r/R_o$, where $\Lambda = \mu B_o/\epsilon$, and that $2\chi^2 R_o/r \approx 1 + r/R_o - \Lambda$ when $a = 0$. When $a > 8|\omega_o - 1|^{3/2}$ the resulting orbits ("quasi bananas") correspond to the representation in Fig. VII-9. In particular, different orbits correspond to different initial conditions. The point P is such that $OP \sim 2a^{1/3}$ and represents the amplitude that the oscillator would reach in the presence of damping. An

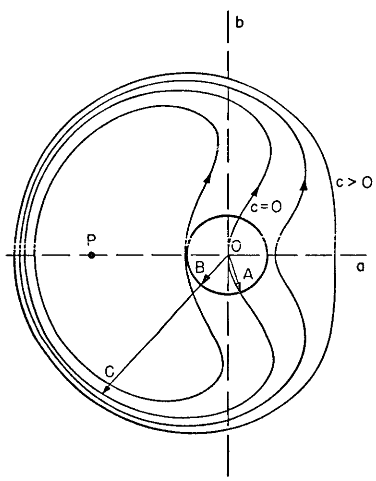

Fig. VII-9. Family of quartics described by Eq. 4 for $(\omega/\omega_{ob}) - 1 < 0$ and different values of the parameter c. An orbit with an amplitude OA at an initial time will develop an amplitude OC if $a \neq 0$. For $(\omega/\omega_{ob}) - 1 > 0$ the resulting quartics have only vertical tangents at the two points intersecting the a axis.

amplitude of the same order of magnitude is obtained, in the absence of damping, when the time average of $\chi^2(t)$ is performed. In particular, this average can be evaluated by the cyclic integral $\oint \chi^2(\psi)\, d\psi$. In conditions of strong resonance, for orbits that are small initially $\left[\theta_o \equiv \theta(t=0) \ll 2a^{1/3}\right]$, we find $\overline{\chi^2} \approx 2a^{2/3}$. Other quantities of interest are the time t_m needed by a small orbit to become large (more precisely to reach the point $\psi \approx \pi/2$), and the time t_M during which the orbit remains large. These quantities can be estimated as $t_m \approx \pi\theta_o/(a\omega_{ob})$ and $t_M \approx 2\pi/\left(a^{2/3}\omega_{ob}\right)$. In conclusion, the small orbits become large in few bounce periods and then they stay large for a longer time, as $t_M > t_m$.

A survey of the even modes[9,10] that can be excited in the limit $\omega \lesssim \langle\omega_b\rangle_i$ points to those which can be associated with the toroidal magnetic field curvature drift of the guiding centers. The eigenfunctions $\tilde{\phi}_m(\theta)$, which characterize these modes, are peaked in the region where the magnetic curvature is favorable. Therefore the effect on the mode stability of trapped particles with large excursion angle tends to prevail over that of the trapped particles with small excursion angle, which are subject to unfavorable magnetic curvature. This is indicated by a quadratic form, which can be derived by substitution from Eq. 2, and can be written as

$$\pi(2/m_i)^2 \int d\epsilon d\mu\, f_{M_i} |2\pi/\omega_{bi}| \left[\sum_{p\neq 0} |\tilde{\Phi}_m^{(p)}|^2 \omega^2 - T_e \omega_{*i} \omega_{Di}^{(0)} |\tilde{\Phi}_m^{(0)}|^2 / T_i \right]$$

$$+ i\omega^4 \omega_{*i}/(4\pi^{5/2}) \int d\lambda \left(L_o^4(\lambda)/v_{thi}^3 \right) \sum_{p\neq 0} |\tilde{\Phi}_m^{(p)}(\lambda)|^2 / |p|^3, \tag{7}$$

where $\omega_{Di}^{(0)} = (1/\tau) \oint d\ell\, \omega_{Di}/|v_{\parallel}|$, and $\omega_{Di} = n^o (d\zeta/dt)_D$, with $(d\zeta/dt)_D$ the angular drift velocity arising from magnetic curvature.[1] The presence of a temperature gradient has been omitted for simplicity, and $\langle\omega_D\rangle_i < \omega < \omega_{*i}, \langle\omega_b\rangle_i$. The relevant profile of the eigenfunction $\tilde{\phi}_m(\theta)$ is such as to make the contribution of the term $\omega_{*i}\omega_{Di}^{(o)}$ positive. It appears impossible to study the influence of these modes on the orbits of trapped particles with relatively large excursions by reducing Eq. 4 to a simple form.

In conclusion, the orbits of trapped ions which in the absence of fluctuations would be "bananas" localized in the region of unfavorable curvature can acquire a considerably large amplitude and reach the region where the magnetic curvature is favorable when the modes with $\omega \lesssim \langle\omega_b\rangle_i$ are excited. As a result, the average magnetic curvature seen by the majority of trapped particles in their orbits may prevent the appearance of magnetic curvature-driven modes and purely growing modes,[9] with characteristic times considerably longer than $\langle\omega_b\rangle_i^{-1}$.

It may be possible to interact with trapped particles if we attempt to enhance the amplitudes of the considered modes from the outside. There are obvious experimental difficulties for this. An oscillating voltage applied between two probes along the torus could produce the desired excitation locally, thereby enabling the modes to select their own toroidal wave number; however, a radial voltage drop may require too large a current to produce a sufficient electric field inside the plasma. Alternatively, the electric field could be created by induction, for example, by a local bar system, but could still suffer an appreciable radial voltage drop.

We are indebted to L. Th. Ornstein and J. Rem for many friendly discussions.

B. Coppi, E. Minardi, D. C. Schram

References

1. J. Callen, B. Coppi, R. Dagazian, R. Gajewski, and D. Sigmar, Paper F-9 in Plasma Physics and Controlled Nuclear Fusion Research 1971, Vol. II (International Atomic Energy Agency, Vienna, 1972), pp. 451-477.
2. B. Coppi, Nuovo Cimento 1, 357 (1969).
3. B. Coppi, M. Rosenbluth, and R. Sudan, Ann. Phys. 55, 207 (1969).
4. L. A. Artsimovich, A. V. Glukhov, and M. P. Petrov, Zh. Eksp. Teor. Fiz. Pis. Red. 11, 449 [Sov. Phys. – JETP Letters 11, 304 (1970)].
5. A. A. Galeev, V. N. Oraevskii, and R. Z. Sagdeev, Zh. Eksp. Teor. Fiz. 44, 903 (1963) [Sov. Phys. – JETP 17, 615 (1963)].
6. The relatively mild temperature gradient required by Eq. 3 is such that the relevant instability can take place well inside the plasma column where the density is not too low. This, combined with the fact that the instability transverse wavelengths can be relatively long, leads one to expect a considerable thermal-energy transport, contrary to the conclusions expressed by B. Coppi, M. Rosenbluth, and R. Z. Sagdeev, Phys. Fluids 10, 582 (1967).
7. M. Rosenbluth, R. Hazeltine, and F. Hinton, Phys. Fluids 15, 116 (1972).
8. R. A. Struble, Nonlinear Differential Equations (McGraw-Hill Book Company, Inc., New York, 1962).
9. B. B. Kadomtsev and O. P. Pogutze, Zh. Eksp. Teor. Fiz. 51, 1734 (1966) [Sov. Phys. – JETP 24, 1172 (1972)].
10. M. Rosenbluth, D. Ross, and D. Kostomarov, Nucl. Fusion 12, 3 (1972).

2. CAN ALCATOR REACH THE BANANA REGIME?

Introduction

Although it is hoped that the feasibility of the Alcator technological principle[1] will soon be demonstrated, the long-range significance of this experiment lies in the study of toroidal plasmas in the "banana regime." The study of trapped-particle effects on neoclassical and anomalous transport is paramount to the success of the use of Tokamaks as fusion reactors. It is therefore of interest to delineate the operational parameters required to produce a "long mean-free path" plasma in machines such as Alcator. The results presented in this report are sufficiently general to be of interest for other Tokamak experiments.

Following, for example, Kadomtsev and Pogutse,[2] we find that the condition for reaching the banana regime is $\nu^{90°} < \epsilon^{3/2}\hat{\omega}_{tr}$, where the inverse aspect ratio $\epsilon = r/R$, the transit frequency $\hat{\omega}_{tr} = v_{th}/Rq$, the "safety factor" $q = rB_{tor}/RB_{pol}$, and $\nu^{90°} = (\tau^{90°})^{-1}$ is the 90° scattering frequency. We define

$$\left.\begin{aligned} X_e &\equiv \epsilon^{3/2}\,\omega_{tr}^{e}\,\tau_e^{90°} \\ X_i &\equiv \epsilon^{3/2}\,\omega_{tr}^{i}\,\tau_i^{90°} \end{aligned}\right\} \tag{1}$$

and delineate the loci $X_e = 1$, $X_i = 1$ in a parameter space spanned by ϵ, $T_{e,i}$, n, z, assuming that R and an average value for q are given (z is the ion charge number). For the collision times we take Braginski's[3] definitions:

$$\tau_e = \frac{3\sqrt{m}\, T_e^{3/2}}{4\sqrt{2\pi}\, nz^2 e^4 \ln \Lambda}$$

$$\tau_i = \frac{3\sqrt{M}\, T_i^{3/2}}{4\sqrt{\pi}\, nz^4 e^4 \ln \Lambda}.$$

The extra z^2 applies if both the scattered and the scattering ion have charge z. More realistically, assuming a hydrogen plasma containing impurities with z_{eff} of 2-4 (cf. the Princeton ST results[4]), we take

$$\tau_e = \frac{3\sqrt{m}\, T_e^{3/2}}{4\sqrt{2\pi}\, nz_{eff}^2 e^4 \ln \Lambda} \tag{2a}$$

$$\tau_i = \frac{3\sqrt{M}\, T_i^{3/2}}{4\sqrt{2\pi}\, nz_{eff}^2 e^4 \ln \Lambda}, \tag{2b}$$

so that

$$\frac{\tau_i}{\tau_e} = \sqrt{\frac{M}{m}} \left(\frac{T_i}{T_e}\right)^{3/2}. \tag{2c}$$

We find it convenient to scale T_e by the electron rest energy (511 keV) and R by the classical electron radius,

$$r_e = \frac{e^2}{mc^2} = 2.8 \times 10^{-13} \text{ cm}.$$

Then, with $T_e = mv_e^2/2$,

$$X_e = \epsilon^{3/2} \frac{v_e^4}{Rq} \frac{3}{16\sqrt{\pi}} \frac{m^2}{nz^2 e^4 \ln \Lambda}$$

$$= \frac{\epsilon^{3/2}(3/16)\sqrt{\pi})\,(2/511)^2 \left(T_e^{\text{keV}}\right)^2}{2.8^2 \times 10^{-26}\, nRqz_{eff}^2 \ln \Lambda}.$$

We take $\ln \Lambda \approx 20$ and obtain

$$X_e(r) = \epsilon^{3/2} \frac{\left(T_e^{\text{keV}}\right)^2}{\hat{n} R q z_{\text{eff}}^2} 1.03 \times 10^5 \tag{3}$$

and

$$X_i(r) \equiv \epsilon^{3/2} \hat{\omega}_{tr}^i \tau_i = \frac{v_i}{v_e} \frac{\tau_i}{\tau_e} X_e = \left(\frac{T_i}{T_e}\right)^2 X_e. \tag{4}$$

Here, $\hat{n}$ is measured in units of $10^{13}/\text{cm}^3$ and R in cm. This shows the strong dependence of the banana-regime criteria $X_{e,i} > 1$ on the minor radius $r = \epsilon R$. In fact, there will always be an inner region which is in the plateau regime.

Results

For Alcator, R = 54 cm, $0 < r/R \leq 0.185$. We assume an average q = 2.5 and also average values for n and T. Figure VII-10 shows T_e vs ϵ (from $X_{e,i} = 1$, Eqs. 3, 4), for $n = 10^{13}$, 10^{14}, $z_{\text{eff}} = 1, 4$.

For the electrons, Fig. VII-10 depicts the function

$$T_e^{\text{crit}} = z_{\text{eff}} \sqrt{\hat{n}/\epsilon^{3/2}} \sqrt{Rq/1.03 \times 10^5}$$

$$= z_{\text{eff}} \hat{n}^{1/2} \epsilon^{-3/4} \, 0.0362. \tag{5}$$

To find the corresponding curves for the ions, we see from (4) and (3) that

$$X_i = \epsilon^{3/2} \frac{\left(T_i^{\text{keV}}\right)^2}{\hat{n} R q z_{\text{eff}}^2} 1.03 \times 10^5,$$

so that the boundary $X_i = 1$ is given by

$$T_i(\epsilon)^{\text{crit}} = z_{\text{eff}} \sqrt{\hat{n}/\epsilon^{3/2}} \sqrt{Rq/1.03 \times 10^5} = T_e^{\text{crit}}(\epsilon). \tag{6}$$

Therefore, as long as the main ion species is assumed to be hydrogen (z = 1), the curves in Fig. VII-10 can also be used to determine the ion regime. If $z_{\text{ion}} > 1$, however, z_{ion}

times the z = 1 temperature is needed for the ion species to reach the banana regime.

Discussion

a. Room-Temperature Operation of Alcator (B = 30 kG, plasma radius, 10 cm).

According to Lidsky and Lecomte,[5] we expect

For $n = 10^{13}/cm^3$: $T_e \sim 1.8$ keV, $T_i \sim 0.2$ keV,

For $n = 10^{14}/cm^3$: $T_e \sim 0.39$ keV, $T_i \sim 0.33$ keV.

Then, from Fig. VII-10, for $z_{eff} = 1$, all of the electrons and half of the ions are in the

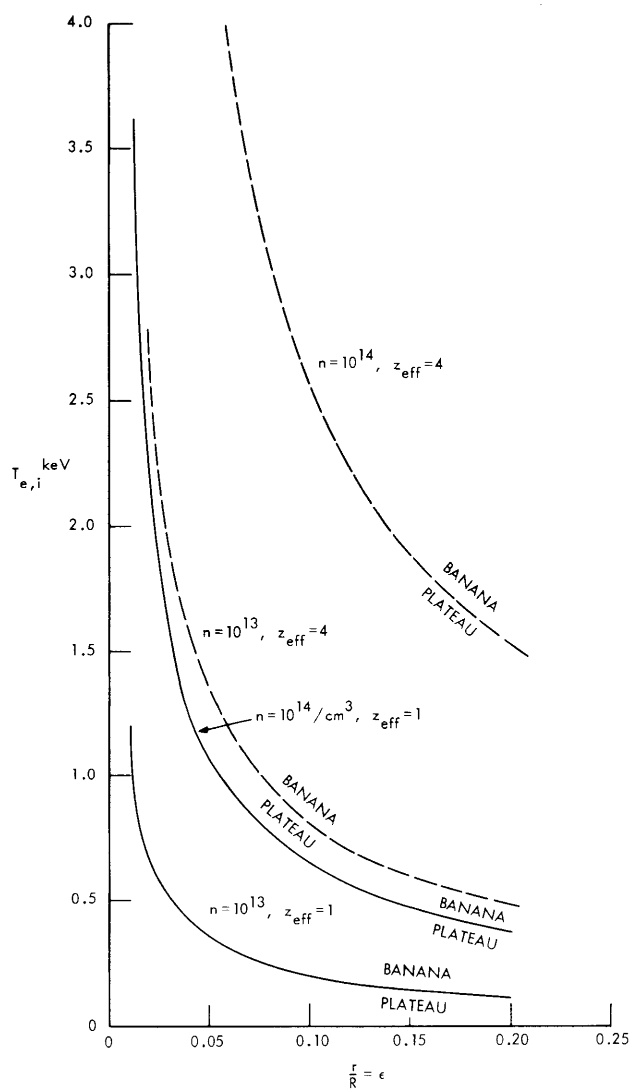

Fig. VII-10. Radial extent of plateau and banana regimes, with hydrogen as the main ion species. (q = 2.5, R = 54 cm.)

banana regime. For $z_{eff} = 4$, 80% of the electrons, but none of the ions, are in the banana regime.

b. Liquid Nitrogen Operation of Alcator ($B \sim 100$ kG).

We expect

For $n \sim 10^{14}/cm^3$: $T_e \sim 4$ keV, $T_i \sim 2$ keV.

From Fig. VII-10, for $z_{eff} = 4$, somewhat surprisingly, only the outer 1/3 of the ion plasma is in the banana regime, even at $T_i = 2$ keV.

General Remarks

1. The values $z_{eff} = 1, 4$ are the most optimistic and the most pessimistic limits, respectively.

2. For more accurate results, the average values of $T_{e,i}$, q, and z_{eff} should be replaced by their radial profiles. For example, the Princeton ST results indicate for z_{eff} a variation from $\gtrsim 3$ at $r = 0$ to 2 at the plasma edge.

3. Since the temperature falls off with radius, Fig. VII-10 should be used with $T_{e,i}$ lower than the average value to determine the plasma regime, near the edge.

4. Overall these curves point to the overwhelming importance of achieving the highest possible ion temperatures. Unless the ions can be taken into the banana regime, extrapolations of present results to reactor-type plasmas will remain uncertain.

D. J. Sigmar

References

1. B. Coppi, "Alcator Experiment," Quarterly Progress Report No. 97, Research Laboratory of Electronics, M.I.T., April 15, 1970, pp. 50-60.
2. B. B. Kadomtsev and O. P. Pogutse, Nucl. Fusion 11, 67 (1971).
3. Reviews of Plasma Physics, Vol. 1 (Consultants Bureau, New York, 1966).
4. D. Dimock et al., Paper CN-28/C-9, IAEA Meeting, Madison, Wisconsin, 1971.
5. L. M. Lidsky and M. A. Lecomte, Private communication, Research Laboratory of Electronics, M.I.T., 1972.